

Thesis for the Degree of Doctor of Philosophy

**Road climate studies with emphasis on road surface  
temperature variations and hoar frost risk**

Yumei Hu



UNIVERSITY OF GOTHENBURG

University of Gothenburg

Department of Earth Sciences

Gothenburg, Sweden 2018

Yumei Hu

Road climate studies with emphasis on road surface temperature variations and hoar frost risk

ISBN: 978-91-7833-063-8 (PRINT)

ISBN: 978-91-7833-064-5 (PDF)

Internet ID: <http://hdl.handle.net/2077/56162>

Printed by BrandFactory, Gothenburg

Copyright © Yumei Hu 2018

Distribution: Department of Earth Sciences, University of Gothenburg, Sweden

## ABSTRACT

An effective road transportation system is a key enabler for national and global economic growth. In the wintertime, the presence of snow and ice on road surfaces reduces road surface friction and can result in serious injuries and significant economic loss. Accurate road weather forecasting, focusing on when and where road slipperiness will occur, improves the efficiency of winter road maintenance activities, thus helping to ensure the safety and mobility of road users. The purpose of this thesis is to increase the understanding of the spatial distribution of road surface temperature (RST) and hoar frost, a common and hazardous form of road slipperiness, across a road network. The thesis consists of two parts. The first part models the influence of geographical parameters on RST distribution during times of day when most traffic uses the road network, using thermal mapping data recorded at times of day other than the latter part of the night. Using thermal mapping from times of day other than the latter part of night makes it possible to assess the feasibility of using road weather related measurements from in-car sensors (Floating Car Data) to model RST distribution. The second part of the thesis characterises the risk of hoar frost on winter roads, across the whole of Sweden, and investigates how that risk changes in a warming climate.

The results show that using thermal mapping from times of day other than the latter part of night, can improve the modelling of RST variation across a road network. Cumulative direct short-wave radiation model that takes shading into account can explain up to 70% of the observed variation in RST and is recommended for daytime RST modelling, due to its simplicity. However, the influence of sky-view factor ( $\psi_s$ ) should not be ignored in the early morning, late afternoon, or when the influence of cloud is significant, because diffuse and long-wave radiation under such conditions play a more important role. Geographical parameters combined with thermal mapping from times of day other than the latter part of night can be used to build repeatable geographical models and explain up to 67% of the variation in RST distributions. The results suggest it might be inappropriate to use air temperature ( $T_a$ ) from Floating Car Data to reflect the influence of geographical parameters on RST distributions. The influence of altitude and the urban heat island might be reflected in the relationship between  $T_a$  and geographical parameters. However, the influence of other parameters, such as shading and ( $\psi_s$ ), is less easy to deduce using  $T_a$  readings from Floating Car Data.

The results in the second part of the thesis show hoar frost is mainly caused by warm air advection in northern Sweden and radiative cooling in southern Sweden. Over the past few decades, increased RST has reduced the risk of hoar frost in the south of Sweden (south of 59°N), whilst increased relative humidity has increased the risk of hoar frost in central Sweden (59°N ~ 65°N). The strengthened winter North Atlantic Oscillation is the main cause for the changes. A warming climate also influences how frequently the conditions that lead to the formation of hoar frost occur. The relative frequency of hoar frost occurring because of warm air advection has significantly decreased, while the relative frequency due to radiative cooling has significantly increased, mainly due to the weakened temperature gradient between land and ocean in a warming climate.

**Keywords:** road climate, road surface temperature, thermal mapping, geographical parameter, air temperature, Floating Car Data, hoar frost, climate change, Sweden

## PREFACE

This thesis includes the following four papers:

- I. **Hu Y.**, E. Almkvist, F. Lindberg, J. Bogren, T. Gustavsson, 2016: The use of screening effects in modelling route-based daytime road surface temperature. *Theoretical and Applied Climatology*, 125:303. <https://doi.org/10.1007/s00704-015-1508-9>. *Y. Hu carried out most of the field measurements and had the main responsibility for data analysis and writing.*
- II. **Hu Y.**, Almkvist E., T. Gustavsson, J. Bogren, 2018: Preparing for Floating Car Data (FCD) as input to a road weather forecast model. *Submitted to Journal of Applied Meteorology and Climatology*. *Y. Hu carried out most of the field measurements, had the main responsibility for data analysis and contributed to the bulk of the writing.*
- III. **Hu Y.**, T. Ou, J. Huang, T. Gustavsson, J. Bogren, 2018: Winter hoar frost conditions on Swedish roads in a warming climate. *International Journal of Climatology*. DOI: 10.1002/joc.5672. *Y. Hu had the main responsibility for data analysis and writing. Pending publication. Printed with permission from the journal.*
- IV. Ou T., **Y. Hu**, T. Gustavsson, J. Bogren, 2018: On the relationship between the risk of hoar frost on roads and climate change in Sweden. *Submitted to International Journal of Climatology*. *Y. Hu contributed to the planning, data analysis and writing of the paper.*

Peer reviewed papers not included in this thesis

Klingberg J., P.E. Karlsson, G.P. Karlsson, **Y. Hu**, D. Chen, H. Pleijel, 2012: Variation in ozone exposure in the landscape of southern Sweden with consideration of topography and coastal climate. *Atmospheric Environment* 47:252-260.  
<https://doi.org/10.1016/j.atmosenv.2011.11.004>.

Conference proceedings and abstracts

**Hu, Y.**, T. Gustavsson, J. Bogren, 2012: Route-based winter road weather forecasting method by using GIS. Proceedings of 16<sup>th</sup> International Road Weather Conference, 23-25 May, 2012, SIRWEC, Helsinki, Finland.

**Hu, Y.**, J. Bogren, T. Gustavsson, E. Almkvist, 2014: Influence of the accumulated screening effect on road surface temperature distribution. Proceedings of 17<sup>th</sup> International Road Weather Conference, 30<sup>th</sup> January – 1st February, 2014, SIRWEC, La Massana, Andorra.

# TABLE OF CONTENTS

INTRODUCTION.....	1
Background .....	2
Aim of the thesis .....	8
DATA AND METHODOLOGY .....	9
Datasets .....	9
Methods .....	12
RESULTS.....	16
Influence of geographical parameters on RST distribution.....	16
Winter road hoar frost risk in Sweden.....	21
DISCUSSION.....	29
Influence of geographical parameters on RST distribution.....	29
Winter road hoar frost risk in Sweden.....	30
CONCLUSIONS .....	34
ACKNOWLEDGEMENTS.....	35
REFERENCES .....	37

## ABBREVIATIONS

DEM – digital elevation model

DSM – digital surface model

FCD – Floating Car Data

$I$  – instantaneous incoming direct short-wave radiation

NCDC – National Climatic Data Centre

$n_{HR}$  – number of hoar frost risk days

$Q^*$  – net radiation

$r$  – Partial Correlation Coefficient

$R$  – Pearson Correlation Coefficient

RH – relative humidity

RST – road surface temperature (°C)

RWIS – road weather information system

SMHI – Swedish Meteorological and Hydrological Institute

$S_r$  – shading ratio

STA – Swedish Transport Administration

$T_a$  – air temperature (°C)

$T_d$  – dew point temperature (°C)

WRM – winter road maintenance

$\psi_s$  – sky-view factor

## **Part I**

### Summary





## INTRODUCTION

A well-functioning transportation system is of significant importance for economic growth both nationally and globally (Eddington, 2006). Of all the factors affecting a transportation system, weather is one of the most important. In cold regions with long winter seasons, severe winter weather events pose particular challenges to the transportation system and may result in serious economic loss to society (Grout *et al.*, 2012).

Slippery road conditions, such as snow and ice, influence the transportation system in terms of both safety and mobility. For instance, Norrman *et al.* (2000) indicated that of all the traffic accidents which occurred during three winter periods in Halland, Sweden, about 50% were related to slippery road conditions. In order to ensure the safety and mobility of road users in the wintertime, winter road maintenance (WRM) activities are required in order to keep winter roads free from slipperiness. In cold regions, annual WRM expenditure can be very high. For instance, the annual winter expense in WRM for Sweden is around 1.7 billion SEK (Swedish Transport Administration, 2015, 2016, 2017). Moreover, the frequent use of road salt in WRM activities, particularly de-icing, can damage the environment and contaminate the ground water (Huling and Hollocher, 1972; Blomqvist and Folkesson, 2001). One way to reduce the negative consequences associated with de-icing is to perform anti-icing, which typically uses three times less salt than de-icing (Thornes, 1991). Thus, effective anti-icing is dependent on accurate predictions of when and where slipperiness will occur. In other words, accurate predictions of road slipperiness can improve the effectiveness of anti-icing and therefore be beneficial to road users and the environment.

Road weather forecasts are usually based on one-dimensional heat balance models, which output predictions of road surface temperature (RST) and road surface condition (amounts of water, snow and ice on the road surface), as illustrated in Figure 1. The prediction of road slipperiness largely depends on the prediction of RST, since it is often a key parameter in determining road slipperiness (Norrman, 2000). Usually when road slipperiness occurs, RST is less than or equal to zero. Moore (1975) concluded that ice is most slippery at 0 °C. Therefore, information about the spatial distribution of RST in a road network is essential for the accurate prediction of road slipperiness, and methods for determining this distribution need to be carefully investigated.

The overall aim of WRM is to reduce the slipperiness of roads. Therefore, it is important to understand the formation conditions, spatial distribution and temporal changes of road slipperiness. Detailed insights could help to improve the accuracy of road slipperiness predictions. In particular, with the prospect of climate change, the occurrence of road slipperiness may also change. This may lead to changes in the frequency of different WRM activities, such as less snowploughing and more salting. Better understanding of the changes can help WRM personnel better plan maintenance activities and deploy WRM equipment. Proper preparation may not only reduce WRM expenditure but also protect the environment by using less salt. Therefore, there is a need to investigate the formation conditions of road slipperiness in different regions and how they might be affected by a changing climate.

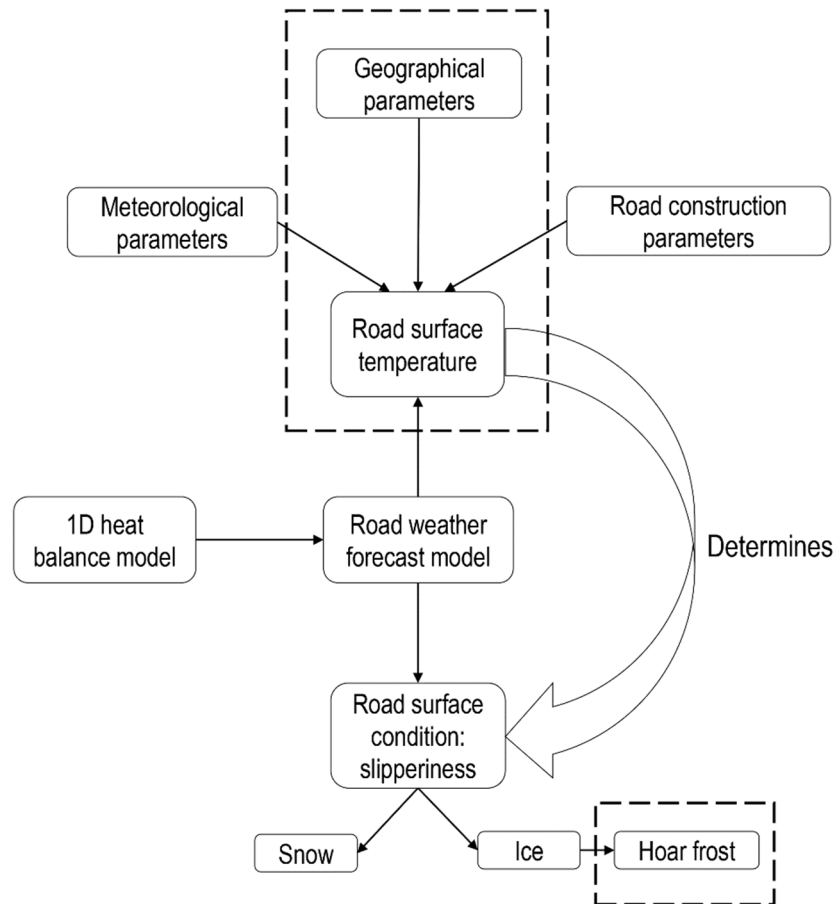


Figure 1. Relationship between road surface temperature and slippery road conditions, with content in the dashed rectangles showing the research directions of this thesis.

## BACKGROUND

### Development of road weather data

Road weather related data are essential for road weather forecasts. Since the 1970s, the means for collecting road weather data has undergone continuous development.

In order to reduce cost of WRM and ensure the safety of road users, the Swedish Transport Administration (STA) established a road weather information system (RWIS) in the mid-1980s. From measurements recorded at roadside weather stations (Figure 2(a)), end users can access data, including air temperature ( $T_a$ ), dew point temperature ( $T_d$ ) and relative humidity (RH) at 2m level, wind speed and direction at 5m level, RST and precipitation information. The collected data is then analysed and used to predict RST and road surface conditions for the next few hours. The number of RWIS stations in Sweden has increased over the last few decades and there are now 775 stations all over the country. However, the density of stations, when compared to the total length of roads, is quite low. Since RST varies even over short distances (Chapman and Thornes, 2011), the observation of RST at RWIS stations might be above zero, while RST for road stretches between the stations has dropped below zero. This might result in slippery conditions between RWIS stations, which is hard to predict using only data from RWIS stations. Therefore, road weather data recorded at points between RWIS stations are needed.



Figure 2. Methods for obtaining road climate data.

Thermal mapping, a technique which uses a moving vehicle mounted with an infrared thermometer (Figures 2(b) and 2(c)) to measure and indicate the spatial variation of RST (Thornes, 1991), provides information about RST variation between RWIS stations. The instrument typically records RST and  $T_a$  at certain intervals e.g. 30m. From the late 1970s, thermal mapping has been used to interpolate RST information between RWIS stations. In order to determine minimum RST and compare RST between different road sections, it is suggested that thermal mapping should be carried out during the latter part of the night (Thornes, 1991), ideally on weekends (Chapman and Thornes, 2005). Using thermal mapping along roads of interest, cold and potentially slippery spots along the roads could be identified. Also, the most suitable locations for RWIS stations could be identified (Lindqvist, 1975, 1976). However, thermal mapping is often time-consuming and costly, which limits its use for the entire road network and prevents it being applied as frequently as RWIS to determine RST.

A cheap and time-efficient road weather data source is needed to improve road weather forecasting. Floating Car Data (FCD) may well provide such a source. Most new cars are equipped with several sensors and devices that are relevant for determining driving conditions, such as air temperature sensors, windscreen wipers (precipitation), ABS brakes (friction estimation) and traction control (friction estimation). Many cars now communicate their data to the cloud in real-time, so this data, if handled properly, could be utilised in a weather forecast model.

Weather-related FCD is likely to be an important Big Data application in the near future. For example, as of winter 2017 – 2018, more than 200 cars in the Gothenburg region deliver data to the cloud, which is used to aid WRM personnel in planning WRM activities. The number of observations from these vehicles is already enormous compared to the number from fixed weather stations. The vehicles cover an area and provide a spatial resolution that are simply infeasible to achieve with fixed stations. If every car in the region were connected to the cloud, the volume of data would increase 100-fold, a true Big Data application, and initiate a new paradigm in road weather forecasting and probably in most weather models.

## RST and geographical parameters

RST, an important parameter for road slipperiness determination, is influenced by many factors, which can be divided into meteorological, geographical, and road construction parameters (Chapman *et al.*, 2001a). The combined influence of these parameters can lead to variation of

nocturnal RST up to 10 °C across a road network within a county (Shao *et al.*, 1996). Variation in geographical parameters across the road network influences the spatial distribution of RST even for short distances.

Many geographical parameters influence the distribution of RST across a road network. This thesis focuses on the influence of shading, hemisphere blocking, altitude, topography and urban heat island. Shading mainly influences the shortwave radiation at the road surface and shaded areas are more likely to experience ice-forming conditions than open areas (Milloy and Humphreys, 1969). Sky-view factor ( $\psi_s$ ), which ranges from 0 (fully obscured) to 1 and measures the degree to which the sky is obscured by the surroundings at a given location, is often used to evaluate the influence of hemisphere blocking on nocturnal radiation budgets (Thornes, 1991; White *et al.*, 2006). The obstructed outgoing long-wave radiation at locations with low  $\psi_s$  values often leads to higher temperatures than in open areas (Geiger *et al.*, 1950), while other studies showed that temperatures at sites with low  $\psi_s$  values was lower than open areas, due to the wind shelter effect (Karlsson, 2000). The influence of altitude on RST is shown in the environmental lapse rate, which varies between 6.5 and 9.8 °C per 1000m (Tabony, 1985). Topography often influences the RST distribution during clear, calm nights, when, for example, cold air pools at the bottom of a valley and results in lower temperature. Urban heat island is defined as the urban canopy area and is usually warmer than the surrounding rural areas (Oke, 1987). Higher RST is often found in urban areas (Gustavsson *et al.*, 2001).

Different geographical parameters often have concurrent influence on the RST distribution. Successful modelling of the combined influence of these parameters may be used for RST interpolation between stations, thereby reducing the need for expensive thermal mapping (Chapman *et al.*, 2001a). Due to the large variation of RST even over short distances, it would be desirable to model the influence of geographical parameters on route-based RST. The models are often developed and tested using thermal mapping data (e.g. Chapman *et al.*, 2001a; Chapman and Thornes, 2006).

Many studies have used thermal mapping data to investigate the influence of geographical parameters on RST (Bogren and Gustavsson, 1991; Gustavsson and Bogren, 1991; Shao *et al.*, 1997; Gustavsson *et al.*, 1998; Gustavsson, 1999; Bogren *et al.*, 2000; Chapman *et al.*, 2001a; Brown *et al.*, 2008). Most of the thermal mapping data was collected at night, typically between 01:00-05:00 (local time) (Chapman *et al.*, 2001a), when the road surface was sufficiently cooled and the influence of incoming short-wave radiation during the day was minimized. This facilitates the comparison of RST between different stretches of road. It is customary to conduct thermal mapping surveys on clear, calm nights, when the amplitude of RST is often large (Chapman & Thornes, 2005). The multiple regression models based on the relationship between late night thermal mapping surveys and different geographical parameters are successful and could explain up to 75% of the observed variation in night time RST distribution (Chapman *et al.*, 2001a).

However, the spatial pattern of RST may look very different at other times and other weather conditions, especially during daytime. Although the daily minimum temperature often occurs just before dawn, it is still very important to understand the RST distribution during other times of the day, when roads experience greater volumes of traffic. Geographical models based on

late night thermal mapping may not explain the RST distribution at other times of the day equally well. Due to the influence of solar radiation, road usage and different weather patterns, the geographical parameter with largest influence on RST may be different during the day. Therefore, it would be desirable to understand the influence of geographical parameters on RST distribution when roads experience greater volumes of traffic and build geographical models based on that. Successful modelling would help to understand the spatial distribution of route-based RST at the time when more vehicles are using the road. In this way, the potential benefit is largest for road users. One key factor in achieving this goal is the ability to capture repeatable thermal fingerprints – the spatial variation of RST plotted against distance for a particular route (Thornes, 1991) – and to use these fingerprints to construct stable geographical models.

In order to build geographical models for RST distribution for times of day other than the latter part of the night, the influence of shading and  $\psi_s$ , which affects the radiation fluxes at the road surface, often needs to be considered. This is due to the increased influence of shortwave radiation at times other than the latter part of the night. Previous studies (Chapman *et al.*, 2001b, c) showed that it is possible to use fish-eye images to calculate shading effects and use them for route-based RST modelling. However, the method is time-consuming, since many fish-eye images need to be collected across the road network for robust analysis to be possible. The availability of the high resolution digital surface model (DSM) derived by light detection and ranging (Lidar) in recent years provides a new, cheaper, less time-consuming and more convenient method of modelling the influence of geographical parameters on RST. Parameters that influence radiation fluxes at the road surface can also be calculated from DSM data (Figure 3), which provides the opportunity to improve the modelling of daytime RST distribution.

In addition, thermal mapping data from times of day other than latter part of night can be analysed as though they are FCD, which are mostly recorded during daytime. In this way, the possible use of FCD in road weather forecasting can be investigated.

### **Hoar frost – a common and hazardous cause of road slipperiness**

Based on ice-forming processes and the characteristics of snow cover, winter road slipperiness can be divided into 24 different types (Lindqvist, 1979; Lindqvist and Mattsson, 1979). Of these types, hoar frost (Figure 4), which forms on the road surface as a result of direct desublimation and reduces surface friction (Karlsson, 2001), is the cause of high accident rates in Sweden compared to other road conditions (e.g. Wallman and Åström, 2001). Hoar frost was responsible for approximately 24% of all traffic accidents in Sweden during the winters of 2004, 2005 and 2006 (Andersson and Chapman 2011), and for about 31% in south-west Sweden between 1991 and 1996 (Norrman 2000). Another problem related to hoar frost is false warmings of the occurrence which will result in excess usage of salt. Improvements in the accuracy and reliability of predictions of hoar frost can lead to considerable savings in energy and costs, and result in more efficient WRM (Riehm and Nordin, 2012).

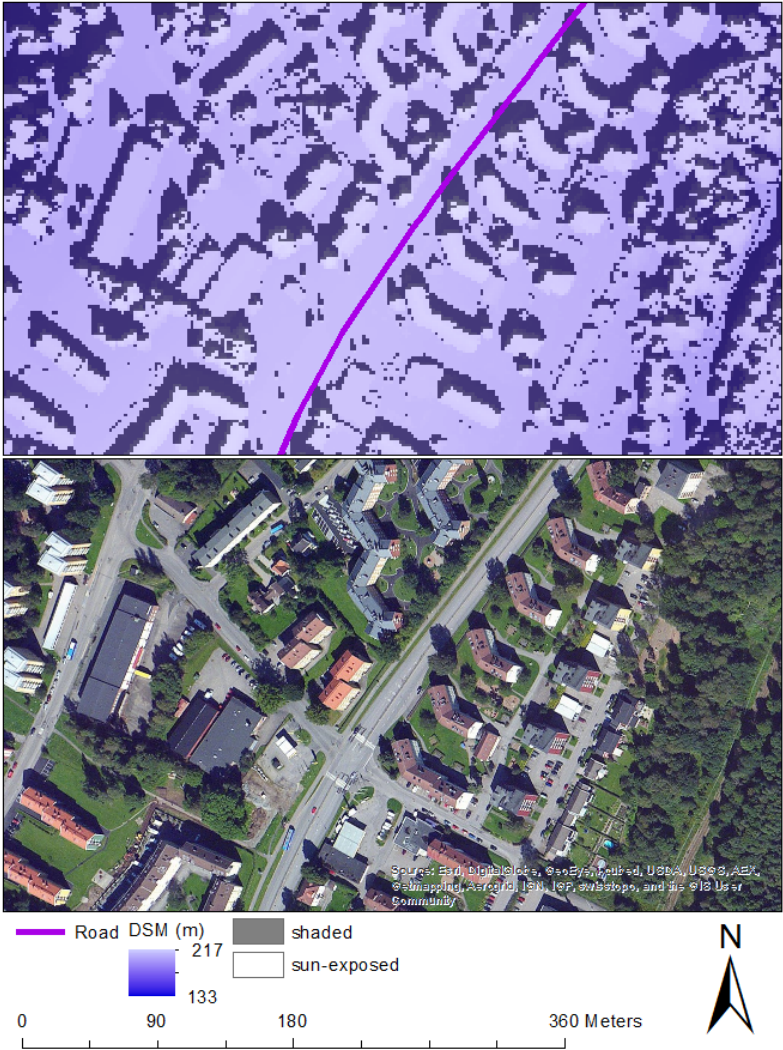


Figure 3. An example of the Lidar data used in this thesis. Figure source: Paper I.



Figure 4. Hoar frost formation on a road surface after a clear night.

Theoretically, hoar frost will form on the road surface when the RST is equal to or less than zero, and  $T_a$  is higher than the RST. The first condition ensures that frost rather than dew will form in association with any moisture deposition; the second condition ensures that moisture flux is directed towards the road surface. Meteorological parameters, including wind speed (Hewson and Gait, 1992; Karlsson, 2001), previous weather conditions (Gustavsson and Bogren, 1990; Takle, 1990; Hewson and Gait, 1992) and the difference between  $T_a$  and RST (Karlsson, 2001), often influence the deposition rate and depth of hoar frost. Of them, wind speed was cited most frequently in previous studies. Karlsson (2001) found that the amount of hoar frost increases with increasing wind speed when wind speed is between 0.11 and 2.13 m/s at 5m level, while Hewson and Gait (1992) suggested that the optimum conditions for the deposition of hoar frost occurs when the wind speed is between 2 and 3.6 m/s at 10m level. It is believed that a wind speed over which the deposition of hoar frost is reduced should exist, due to increased turbulence (Gocheva, 1990). However, that speed is still unknown. Wind speed is also known to affect the formation of dew, and the processes governing the creation of dew and hoar frost are thought to be similar (Oke, 1987). However, Crowe et al. (1978) found that dew still forms on a wheat crop canopy when the wind speed is about 5m/s at 3m level and can remain there for more than 6 hours. In other words, it is hard to estimate the wind speed at which the deposition of hoar frost is reduced on the road surface.

There are three conditions that can lead to the occurrence of hoar frost: 1) warm air advection which is characterized by a warm front passing over a cold surface; 2) radiative cooling which leads to the road surface cooling faster than the air directly above it; and 3) rising air temperature, associated with increasing temperature in the morning, but cold road surfaces (Lindqvist, 1979; Lindqvist and Mattsson, 1979). Of them, warm air advection and radiative cooling are often observed (e.g. Gustavsson and Bogren, 1990; Bogren *et al.*, 2001; Karlsson, 2001) and used to parameterize the forming of hoar frost (e.g. Toms *et al.*, 2017). However, little attention has been paid to the third method of hoar frost formation in the literature.

Over the last few decades, climate change has been reported globally (Stocker et al., 2013; Huang et al., 2017). According to most climate models, one of the main consequences of climate change is an increase in global temperature. Such warming can lead to an increase in RST, which will reduce the occurrence of hoar frost. Bulygina et al. (2015) reported that the occurrence of winter icing and hoar frost decreased with a temperature increase in Russia between 1977 and 2013 based on visual observations. Nevertheless, a warming climate can also enhance the hydrological cycle, which may lead to an increase in RH and the potential for near-surface air to be saturated, increasing the likelihood of hoar frost forming. Sweden has become warmer and wetter over the last few decades. The Swedish Meteorological and Hydrological Institute (SMHI) reports that winter surface air temperature has risen up to 3°C in Sweden between 1991 and 2016 relative to the reference period of 1961 – 1990 (SMHI, 2017). Accompanying the warming, near-surface RH has also risen in Sweden over the last few decades (Dai, 2006; Simmons *et al.*, 2010). Given the different effects changes in temperature and RH have on the likelihood of hoar frost forming, it is necessary to examine the response of winter hoar frost risk to recent climate change. Understanding this response could be useful in predicting the risk of hoar frost in the future and preparing appropriate WRM activities in advance. In addition, this knowledge could also be used by transportation policy-makers

developing road-related infrastructure adaptation strategies, in order to mitigate the effects of climate change. Therefore, it is of great importance to study how hoar frost risk has changed over the last few decades in Sweden and how the change is related to recent climate change.

## **AIM OF THE THESIS**

The overall aim of the thesis is to improve our understanding about how RST and hoar frost risk vary in a road network, which will improve the accuracy of forecasts for RST and road surface conditions. The thesis focuses on the influence of geographical parameters on RST and the influence of climate change on winter road hoar frost risk (Figure 1).

Specific objectives are to:

- Examine the possibility of using thermal mapping recorded at times of day other than the latter part of the night together with geographical parameters in explaining the variation of RST across a road network (Paper I, Paper II).
- Model the influence of route-based screening effects on daytime RST distribution using high resolution Lidar-generated data (Paper I).
- Improve the understanding of how geographical parameters influence RST at times of the day when most daily traffic occurs and examine the possibility of using  $T_a$  from FCD in road weather forecast (Paper II).
- Evaluate the influence of recent climate change on hoar frost risk on Swedish roads (Paper III).
- Characterize the conditions under which there is risk of hoar risk forming in Sweden and investigate its link with recent climate change (Paper IV).



# DATA AND METHODOLOGY

## DATASETS

All studies considered in this thesis were conducted in Sweden: Paper I and Paper II focused on specific routes in south-west Sweden; Paper III and Paper IV included RWIS station data from the whole of Sweden. Multiple datasets were used for the studies. An overview of the datasets is shown in Table 1, followed by a short summary of each category of data. For more detailed information about the datasets, see Papers I-IV.

Table 1. Utilized datasets and study area for each paper.

Paper	Study area	Thermal mapping	RWIS data	Geographical data	Meteorological data
I	Borås	9 runs	RST T <sub>a</sub>	Road vector data Land use	Radiation data from STRÅNG <sup>②</sup>
	E6, north of Gothenburg	7 runs	RH	Lidar generated DSM DEM <sup>①</sup>	
II	Borås	32 runs	RST T <sub>a</sub> Wind speed	Road vector data Land use ÅDT <sup>③</sup> data DEM Lidar generated DSM	Surface sky cover data from NCDC <sup>④</sup> Cloud information from MESAN <sup>⑤</sup>
III	Whole Sweden	/	RST T <sub>a</sub> RH	/	NAO <sup>⑥</sup> index ERA-Interim data
IV	Whole Sweden	/	Precipitation T <sub>d</sub>	/	T <sub>a</sub> at 2m and 850 hPa level and sea level pressure from MERRA-2 <sup>⑦</sup>

①: Digital Elevation Model, ②: a mesoscale model for solar radiation; ③: hourly traffic volume data; ④: National Climatic Data Centre; ⑤: meteorological analysis model; ⑥: North Atlantic Oscillation; ⑦: Modern-Era Retrospective analysis for Research and Applications, Version 2.

### Thermal mapping

In Paper I and Paper II, thermal mapping data collected between 2012 and 2014 were utilized. A vehicle mounted with an infrared thermometer was used to record RST along two routes of interest – one being highway E6 from Kungälv to Nordbymotet overpass, the other comprising three country roads in Borås region – as shown in Figure 5. Most of the surveys were conducted during times of day when most daily traffic occurs. During the course of each survey, T<sub>a</sub> was also recorded at 2m level. Each survey in Borås took around one hour, while some surveys in the highway region took as long as 2 hours. In total 41 surveys were conducted, 34 surveys on the country road and 7 surveys on the highway. As shown in Table 2, different weather conditions were covered. In Paper I, 16 surveys undertaken during clear or partly cloudy conditions were used, while in Paper II, 32 thermal mapping surveys from the same winter season in the Borås region were used. Note that some thermal mapping measurements were used in both Paper I and Paper II, but different ID numbers were used in each case. The corresponding ID number for each thermal mapping survey in each paper is shown in Table 2.

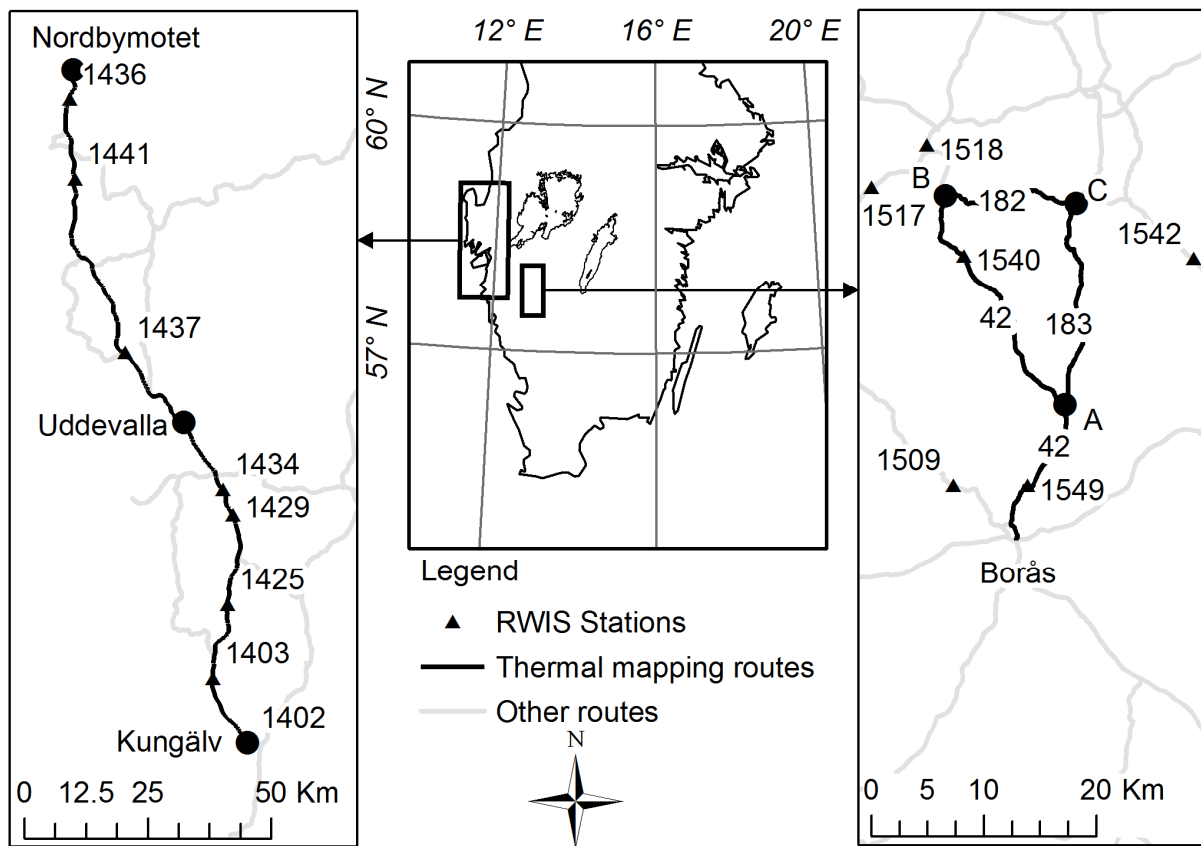


Figure 5. Location of thermal mapping routes and RWIS stations used in Paper I and Paper II. A, B, C are control points during thermal mapping surveys in the Borås region. Figure source: Paper I (modified).

## RWIS data

Observations from RWIS stations were used in each paper. RWIS stations record the meteorological information of the road environment every 30 minutes. Variables used in each paper are shown in Table 1. In Paper I and Paper II, RWIS data recorded by stations close to the studied routes were used to provide weather information, while data from 244 RWIS stations distributed across the whole of Sweden were used in Paper III and Paper IV to calculate the winter hoar frost risk from 1999/2000 to 2015/2016.

## Geographical data

In Paper I and Paper II, geographical data were used to develop geographical parameters. Road vector data, land use data, Lidar-generated DSM data, and DEM data were provided by the Swedish mapping, cadastral and land registration authority (Lantmäteriet), while ÅDT data was provided by STA.

Table 2. Thermal mapping measurements used in this thesis, with measurements from night time shaded. \*: the following day. WS: wind speed at 5m level. Prep: precipitation.

Area	Date	Time	Weather pattern	Cloud	WS (m/s)	ID in Paper I	ID in Paper II
Borås	2012-01-23	11:49-13:00	partly cloudy	0-8	3.7	/	M1
	2012-01-23	14:19-15:30	partly cloudy	7-8	4.2	/	M2
	2012-01-27	10:11-11:21	overcast, prep.	8	8.7	/	M3
	2012-01-27	13:58-15:06	overcast	8	7.6	/	M4
	2012-01-27	16:09-17:20	overcast	8	7.4	/	M5
	2012-02-01	10:30-11:40	partly cloudy	3	2.8	M1	M6
	2012-02-01	14:14-15:29	overcast, prep.	8	3.4	/	M7
	2012-02-01	16:56-18:16	overcast, prep.	8	3.9	/	M8
	2012-02-02	18:21-19:43	partly cloudy	3	4.0	/	M9
	2012-02-02	21:24-22:39	partly cloudy	6	3.0	/	M10
	2012-02-02	23:51-01:04*	partly cloudy	3	3.4	/	M11
	2012-02-06	18:03-19:17	partly cloudy	4	3.4	/	M12
	2012-02-06	20:57-22:11	partly cloudy	4	4.7	/	M13
	2012-02-06	23:45-01:00*	partly cloudy	4	4.8	/	M14
	2012-02-09	10:06-11:18	partly cloudy	4	3.2	/	M15
	2012-02-09	14:00-15:09	overcast	8	11.2	/	M16
	2012-02-09	16:59-18:14	partly cloudy	7	12.7	/	M17
	2012-02-20	18:12-19:31	overcast, prep.	8	10.8	/	M18
	2012-02-20	21:06-22:33	overcast, prep.	8	10.0	/	M19
	2012-02-20	23:58-01:28*	overcast, prep.	8	8.1	/	M20
	2012-02-29	18:01-19:17	clear	0	11.8	/	M21
	2012-02-29	21:04-22:18	overcast	8	5.3	/	M22
	2012-02-29	23:52-01:05*	overcast	8	6.0	/	M23
	2012-03-02	10:26-11:37	clear	0	2.9	M2	M24
	2012-03-02	14:01-15:12	clear	0	5.9	M3	M25
	2012-03-02	17:06-18:16	clear	0	8.5	M4	M26
	2012-03-06	10:05-11:15	partly cloudy	4	4.5	M5	M27
	2012-03-06	14:03-15:14	partly cloudy	4	7.7	M6	M28
	2012-03-06	16:51-18:01	partly cloudy	3	4.0	M7	M29
	2012-03-07	18:01-19:18	overcast	8	5.7	/	M30
	2012-03-07	21:09-22:25	overcast, prep.	8	4.1	/	M31
	2012-03-07	23:46-01:12*	overcast, prep.	8	2.7	/	M32
2014-04-15	15:11-16:29	Clear	0	5.6	M8	/	
2014-04-15	17:13-18:25	Clear	0	5.1	M9	/	
E6	2013-03-11	12:02-13:48	Clear	0	2.3	M10	/
	2013-03-11	13:55-15:41	Clear	0	2.8	M11	/
	2013-03-11	15:49-17:25	Clear	0	3	M12	/
	2014-03-21	11:53-12:40	Clear	0	5.7	M13	/
	2014-03-21	12:53-13:39	Partly cloudy	0-7	7.7	M14	/
	2014-04-04	7:42-8:33	Partly cloudy	3	0.4	M15	/
2014-04-04	9:32-10:23	Partly cloudy	3	2.4	M16	/	

## Meteorological data

Different meteorological data was used in each paper.

In Paper I, hourly global and direct shortwave radiation predictions from the model STRÅNG were used to calculate the radiation reaching the road surface. STRÅNG (Landelius et al. 2001), developed by SMHI, is a mesoscale model for solar radiation, which covers the whole of Sweden. It predicts solar radiation levels with a resolution of  $11 \times 11$  km for all periods since June 2006.

In Paper II, two types of meteorological data were used. The hourly surface sky cover data from two stations, provided by NCDC, were used to calculate the weather pattern conditions in the study area. In addition, the hourly total cloud information with 11 km spatial resolution from the meteorological analysis model MESAN, provided by SMHI, was used to show the cloudiness distribution ahead of and during each thermal mapping.

In Paper III, two meteorological datasets were used to evaluate the influence of climate change on the frequency with which hoar frost occurs. NAO index was extracted from the Climate Prediction Centre (<http://www.cpc.ncep.noaa.gov>). ERA-Interim, global atmospheric re-analysis data, was downloaded from the ECMWF Public Datasets web interface (<http://apps.ecmwf.int/datasets/>). For detailed information, see Dee et al. (2011).

In Paper IV, data from MERRA-2 (Gelaro *et al.*, 2017) were used to analyse the changes in large-scale wind and temperature to understand the changes in hoar frost. Hourly temperature at 2 m and 850 hPa, and sea level pressure are retrieved from MERRA-2 with a horizontal resolution of  $0.5^\circ \times 0.625^\circ$  (Latitude  $\times$  Longitude).

## METHODS

In this thesis, Paper I and Paper II are intended to improve the modelling accuracy of RST by investigating the influence of geographical parameters on RST from thermal mapping surveys undertaken at times of day when relatively more road users were on the road. Segment-based data analysis was used to relate temperatures and geographical parameters in both studies. The radiation fluxes at road surface were generated using radiation output from STRÅNG to model the distribution of daytime RST in Paper I, with the influence of screening effects – a combination of the influence of shading and hemisphere blocking – being taken into consideration. In Paper II, the influence of geographical parameters – including altitude, relative altitude,  $\psi_s$ , shading, and urban density – on RST from thermal mapping surveys undertaken at times of day other than the latter part of the night and the possibility to build a geographical model from the measurements, were examined. In particular, the possibility of using  $T_a$  from FCD to reflect the variation of RST, as a consequence of the interaction of geographical parameters in a road network, was further investigated in Paper II. This was done by examining the repeatability of thermal fingerprints from different thermal mapping surveys and comparing the influence of geographical parameters on RST and  $T_a$  separately.

Paper III and Paper IV are intended to characterize the spatial and temporal distribution of the risk of hoar frost on winter roads in Sweden. In addition, the change in this risk due to a warming

climate and its link with recent atmospheric circulation changes was investigated. The focus was on the risk of winter hoar frost between 1999/2000 and 2015/2016. In these two studies, hoar frost risk was first defined based on theory and practical application. Thereafter, the characteristics of hoar frost, a classification based on the causes of hoar frost, the changes in hoar frost risk and their links with recent climate change, were investigated.

### **Segment-based data analysis**

In Paper I and Paper II, the road vector data were divided into 50-m segments and the thermal mapping data, derived geographical parameters and radiation fluxes were spatially related to the segmented scaled road vertices. This segment-based approach facilitated quantitative analysis of the relationship between geographical parameters and temperatures. A segment length of 50m was chosen to match the scale of thermal mapping.

Most of the geographical parameters, except  $\psi_s$ , were calculated in a geographical information system (GIS) environment. Based on DEM with 2m spatial resolution, altitude and relative altitude, and the altitude difference between the segment and the surrounding area, with 2km searching radius, were calculated. Relative altitude was used to reflect the influence of topography on temperature. Urban density, which is used to reflect the influence of urban heat island on temperature, was calculated based on the land use data with 25m spatial resolution. In order to calculate the urban density, the urban area was first identified and its point density with 1km searching radius in ArcGIS desktop was used for the calculation. For both Paper I and Paper II, a Lidar-generated DSM with spatial resolution 2m and vertical resolution 0.2 m was used to generate parameters including shading and  $\psi_s$ . The shading ratio ( $S_r$ ) measures the proportion of a segment that is shaded and ranges between 0 and 1 (fully shaded). Note that the mean of accumulated shading effect over three hours was calculated and used in Paper II. This is based on the result of Paper I, which will be described later. Sky-view factor was calculated using the solar long-wave environmental irradiance geometry (SOLWEIG) model. Details are described in Paper I.

### **Modelling of radiation fluxes at the road surface**

In Paper I, in order to build radiation models explaining RST variations, the radiation fluxes at the road surface were calculated for each road segment. The radiation fluxes considered are shading influenced fluxes (the incoming direct shortwave radiation), sky-view factor influenced fluxes (the incoming diffuse radiation, the incoming long-wave radiation from the sky, the long-wave radiation reflected from the surroundings to the road surface, the long-wave radiation emitted from the surroundings to the road surface), and fluxes influenced by both parameters (the direct and diffuse radiation reflected from the surroundings to the road surface, the outgoing shortwave radiation reflected from the road surface back to the sky). For detailed equations, see Paper I.

As most of the measurements were conducted over a period of one hour, it was necessary to ensure that the radiation fluxes for each segment were calculated for the time when its RST was recorded, in order to avoid discrepancies between the timing of the RST measurement and the corresponding radiation flux calculation. This was done by simple time-based interpolation,

which was also used to interpolate the RST data from the RWIS stations prior to computing the outgoing longwave radiation flux. To determine how detailed the model needed to be in order to adequately describe the RST distribution along the road, the total incoming radiation, net radiation ( $Q^*$ ), and incoming direct shortwave radiation ( $I$ ) were calculated for each road segment and measurement timing, and compared to the measured RST values.

## **Hierarchical and K – means clustering methods**

This thesis uses the hierarchical binary clustering and the K-means clustering methods, both of which are commonly used for cluster analysis.

In Paper II, the hierarchical binary clustering method was used to examine the repeatability of thermal fingerprints from different thermal mapping surveys. The Pearson correlation coefficient (R) between each pair of thermal mapping runs was calculated and R was used as an input to the clustering algorithm. The cut-off value for R was set to 0.5, which means thermal mapping surveys with R below 0.5 would not be classified into the same cluster. The choice of cut-off should not only ensure thermal mappings in the same group having similar thermal fingerprints, but also produce as few groups as possible, so that thermal mappings with similar thermal fingerprints are not grouped into different groups. A number of different cut-off values were tested and 0.5 was chosen since the results obtained using this value fitted the requirements best. The hierarchical binary clustering method does not require knowledge of the number of clusters. This method was chosen to classify thermal fingerprints, since thermal mapping surveys were conducted at different times and under different weather conditions and it was difficult to determine the number of clusters in advance.

In Paper IV, the K-means algorithm (Wilks, 2011) was used to conduct the cluster analysis and classify the RWIS stations into different zones. Unlike the hierarchical binary clustering method, the K-means clustering requires prior knowledge of the number of clusters. The K-means method is better equipped to handle large amounts of data than the hierarchical method. Given the amount of data used in Paper IV, the K-means method was used for climate zone classification.

## **Defining winter road hoar frost risk**

In this thesis, occurrence of hoar frost is defined as being when there is no precipitation, RST is less than or equal to 0 and  $T_a$  is greater than RST.  $T_a$  is calculated using the following formula, derived from Stull (2000):

$$T_a = \left[ \frac{1}{T_a} - c \times \ln(RH) \right]^{-1} - 273 \quad (1)$$

where  $c = \frac{461}{2830000}$  K,  $T_a$  is air temperature at 2m level and RH is relative humidity at 2m level.

A substantial amount of frost has to be deposited to create slippery road conditions (Knollhoff et al., 2003). In Sweden, traffic is assumed to be adversely affected if road surface friction is

less than 0.4 (Al-Qadi et al., 2002). Karlsson (2001, Figure 3(a)) noted that road surface friction can fall close to 0.4 two hours after the first occurrence of hoar frost. In this thesis, a hoar frost risk day is defined to be one day in which the occurrence of hoar frost lasts longer than 2 hours (four consecutive 30-minute measurements), where a day is defined as being the 24-hour period from 12:00 noon local time.

In Paper III, the number of hoar frost risk days ( $n_{HR}$ ) for each winter was calculated and the decadal trend of winter road hoar frost risk was calculated using least squares regression method, which minimises the sum of the squares of the errors between predicted and observed values. In Paper IV, changes in temperature immediately before an occurrence of hoar frost risk were investigated to characterize the conditions under which hoar frost forms in different regions.

## RESULTS

### INFLUENCE OF GEOGRAPHICAL PARAMETERS ON RST DISTRIBUTION

#### Using screening effects in modelling route-based daytime RST

Paper I shows that the spatial distribution of RST is often closely related to screening effects during daytime. RST on a clear day can be highly correlated with the calculated instantaneous incoming direct short-wave radiation ( $I$ ) reaching the road surface, only with the influence of shading effect considered (Table 3). The calculated instantaneous all incoming radiation or net radiation ( $Q^*$ ) can increase the explained variance of RST in some cases (e.g. cases during early mornings), but not for cases close to sunset. In all cases, the cumulative total incoming radiation,  $I$  and  $Q^*$ , which considered the radiation fluxes prior to the measurements (i.e. the cumulative road surface radiation flux prior to measurement) as well as instantaneous radiation fluxes, explains the RST distribution more fully than the corresponding instantaneous radiation fluxes, due to the heat storage of the roadbed. In the best cases, the explained variance of RST by using cumulative model is improved by 30%.

*Table 3. The correlation coefficient between different instantaneous radiation fluxes and the distribution of RST. Table source: Paper I.*

ID	R		
	$I$	All incoming radiation	$Q^*$
M1	0.37*	0.55*	0.51*
M2	0.72*	0.71*	0.71*
M3	0.74*	0.73*	0.73*
M4	0.17*	0.15*	0.02
M5	0.77*	0.75*	0.73*
M6	0.73*	0.76*	0.76*
M7	0.26*	0.26*	0.05
M8	0.69*	0.68*	0.67*
M9	0.57*	0.51*	0.42*
M10	0.34*	0.40*	0.38*
M11	0.68*	0.69*	0.66*
M12	0.81*	0.81*	0.79*
M13	0.50*	0.49*	0.49*
M14	0.59*	0.63*	0.64*
M15	0.70*	0.75*	0.73*
M16	0.63*	0.66*	0.64*

\*: Correlation is significant at the 0.01 level (2-tailed).

The ability of cumulative models in explaining the observed variation in RST distribution varies with the length of the accumulation period. The optimal accumulation period to maximize the explained variance of RST was associated with the timing of the measurement for both the country road and highway areas (Figure 6). For measurements in the country road area, the later



the RST measurement is taken, the greater the accumulation period required to maximize R, while the accumulation time required to maximize R increases as the timing of the measurement gets closer to noon in the highway area. The difference in the optimal accumulation period is caused by the differences in road environment between the two study areas. It is expected that the relationship between the accumulated radiation and the RST distribution in the country road area is likely to be applicable in many of Sweden's roads, which feature many bends and roadside objects that will create shade. On the other hand, the models developed for the highway area may be applicable in other highway environments in which there are few bends.

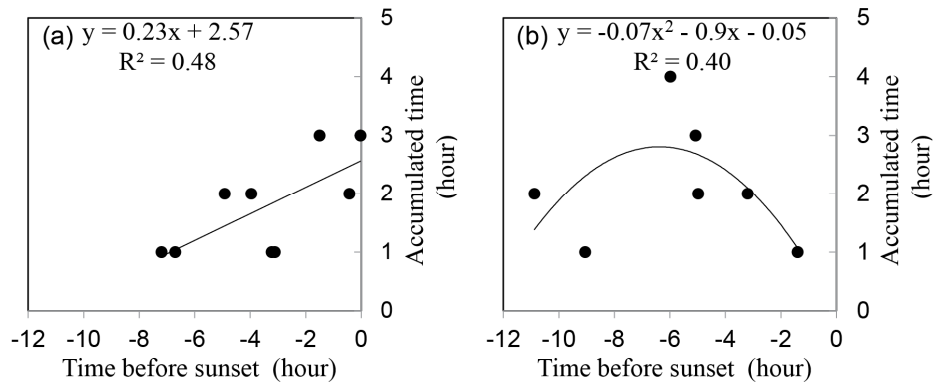


Figure 6. The relationship between the time before sunset (when each measurement was conducted) and the duration of the accumulation period required to maximize R in (a) the country road area and (b) the highway area. Figure source: Paper I (modified).

The cumulative  $I$  values calculated using the shading effect model generally explain the RST distribution well (Figure 7). However, for cases during early morning or late afternoon, the cumulative total incoming radiation and  $Q^*$  model significantly improved the explained variance in RST, which indicates the importance of including  $\psi_s$  when modelling RST variation under such conditions. However, the inclusion of  $\psi_s$  significantly complicates the simulation process because the calculation of  $\psi_s$  and other radiation fluxes is substantially more time-consuming than that of the shading effect and  $I$ .

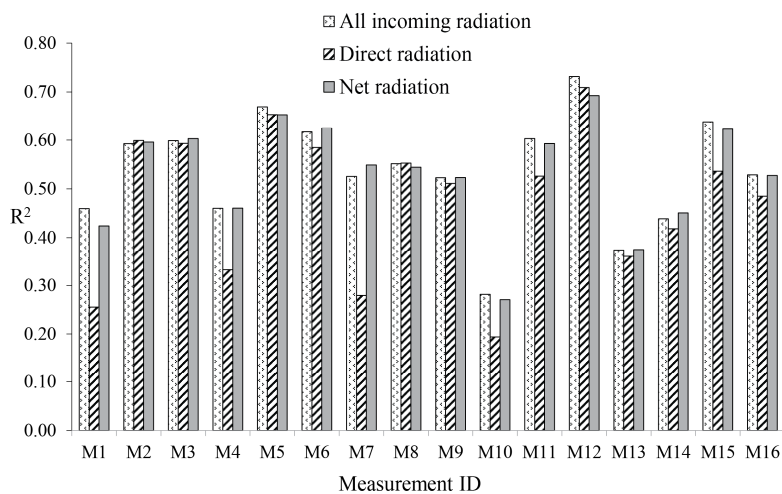


Figure 7. The proportion of the variance in the RST distribution explained using models based on different cumulative radiation fluxes. Figure source: Paper I (modified).

Therefore, a cumulative  $I$  model was built for practical use for each region. The results presented in Figure 6 were used to calculate the optimal accumulation period for each measurement. The model can explain 57% of the spatial variation in the RST for the country road area and 51% for the highway area (Figure 8). Leave-one-out cross-validation was then conducted, the results showing that, in the best cases, the general radiation models explained 65% of the RST variation in the country road area and 71% in the highway area.

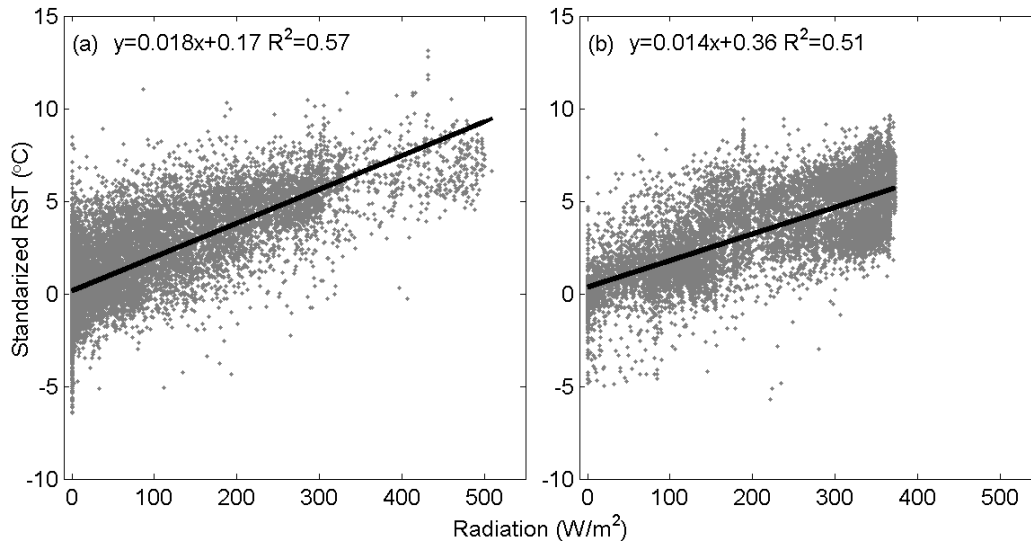


Figure 8. (a) The relationship between the accumulated direct radiation predicted by the general model for the country road area and the corresponding standardized RST values. Radiation denotes the accumulated direct radiation and the standardized RST is the difference between the actual RST along the road and the environmental RST. Subfigure (b) shows the equivalent results for the highway area. Figure source: Paper I (modified).

### Attempt to utilize FCD to reflect route-based RST distribution

From the 32 thermal mapping surveys undertaken on the country road routes at times of the day other than the latter part of the night, repeatable thermal fingerprints (Figure 9) were recorded for late winter morning runs with clear weather conditions (group 1), early winter evening runs with partly cloudy to overcast weather conditions (group 7), late winter runs during different weather patterns and different times (group 9) and early winter runs from evening to late night during partly cloudy weather conditions (group 16). However, for the same weather pattern, when the spatial variation of RST is repeatable, the spatial patterns of  $T_a$  from different surveys are not always similar; indeed the variations can be quite significant. The variations in values of  $T_a$  are often much lower than those for RST.

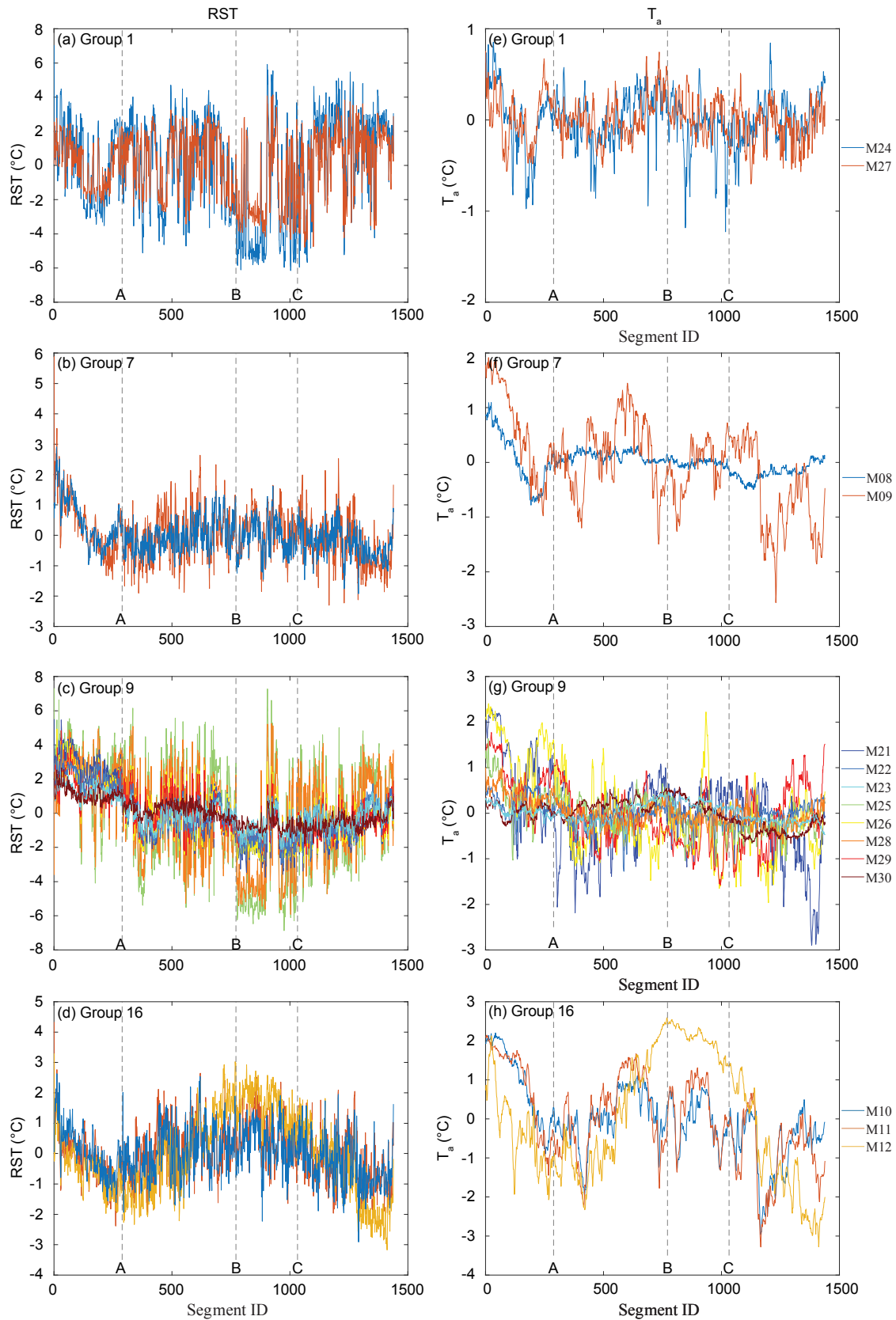


Figure 9. Identified groups of thermal mapping data ((a) to (d)) with repeatable thermal fingerprints, and plots of air temperature based on the group classification. A, B and C show the control point during thermal mapping survey as shown in Figure 5. It needs to be noted that the y-scale are different for RST and  $T_a$ .

The repeatable thermal fingerprints were often measured at similar times of the day or with similar weather patterns, e.g. M25, M26, M28, and M29 in group 9 (Table 2). However, some repeatable thermal fingerprints were recorded during different weather conditions from other surveys in the same group, e.g. overcast. It was found that the preceding weather patterns prior to each thermal mapping survey exerted a strong influence on the spatial pattern of thermal mapping, due to the heat storage of the roadbed. For surveys conducted during overcast weather conditions and close to sunset, the influence of preceding weather up to 12 hours prior to the measurements should be considered. Therefore, in order to classify future thermal mapping measurements into the correct group, first the measurement time and corresponding real-time weather pattern should be checked. Then, the preceding weather pattern should be checked, especially for measurements during overcast conditions.

The influence of individual geographical parameters on RST and  $T_a$  was calculated using the partial correlation method for each group. The results are shown in Figure 10. Different geographical parameters were found to be dominant for different thermal fingerprint groups. Though, it seems that for RST measurements within a group, the dominating parameters are the same, which indicates that it is possible to build repeatable geographical models from thermal mapping surveys undertaken at other times of the day than the latter part of the night in order to improve the modelling of RST.

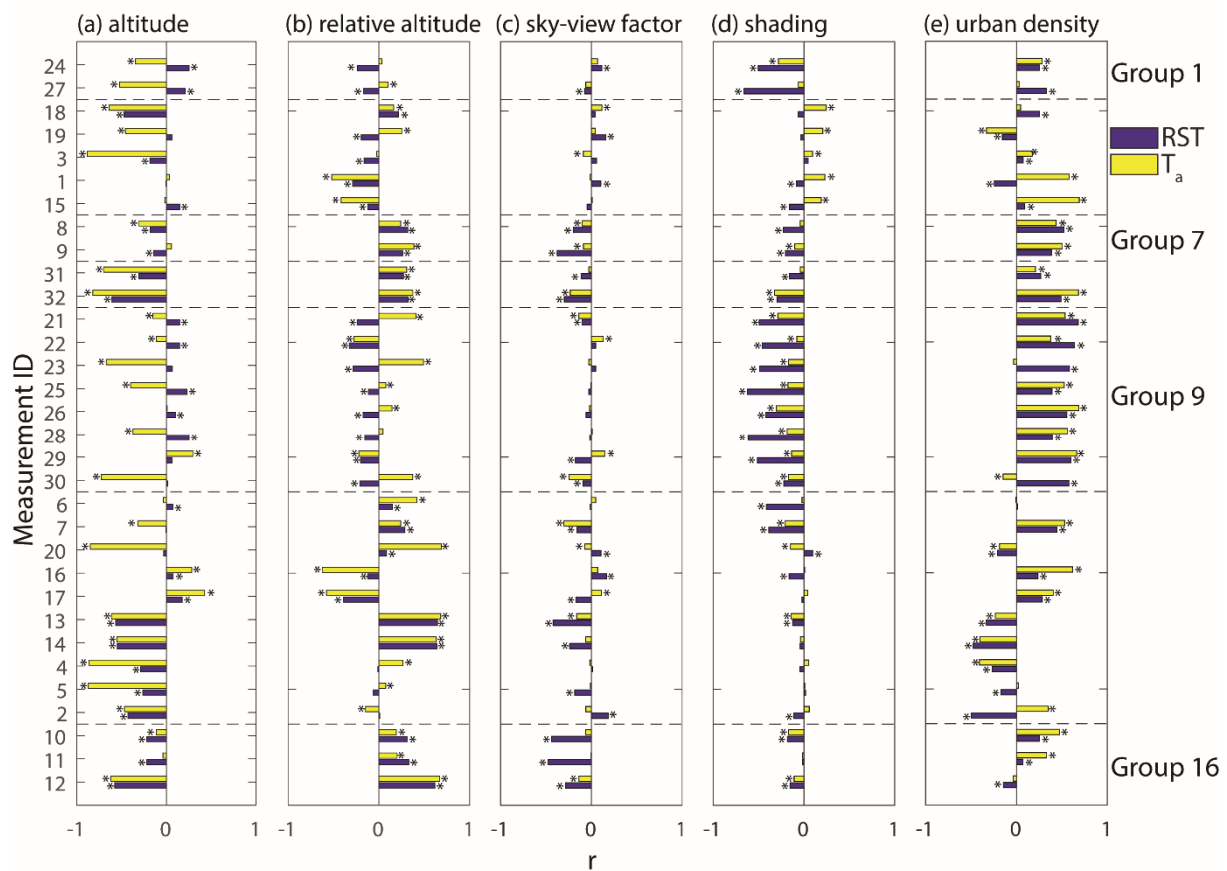


Figure 10. The partial correlation coefficient ( $r$ ) between different geographical parameters and temperatures from different groups. \*: Correlation is significant at the 0.01 level (2-tailed).

However, the influence of geographical parameters on RST is not always seen in the relationships between geographical parameters and  $T_a$ . In general, the influence of urban heat island and altitude on RST is similar to that on  $T_a$ . The influence of shading can also be seen, although it is considerably weaker. No relationship was found between  $\psi_s$  and  $T_a$ . Sometimes,  $T_a$  correlates well with altitude, but no similar relationship could be found between altitude and RST. Unlike the consistent relationships between geographical parameters and RST in the same group,  $T_a$  measurements in the same group can have quite different correlations with the same geographical parameters.

Multiple linear regression geographical models were built for RST and  $T_a$  separately for each survey. As expected, repeatable models were built for RST in the same group with explained variation up to 67%, while the models built for  $T_a$  were not always repeatable, which makes the application of the models to  $T_a$  more questionable.

## WINTER ROAD HOAR FROST RISK IN SWEDEN

In Paper III and Paper IV, the characteristics and classification of winter hoar frost risk on Swedish roads and how they change as a result of the changing climate were investigated.

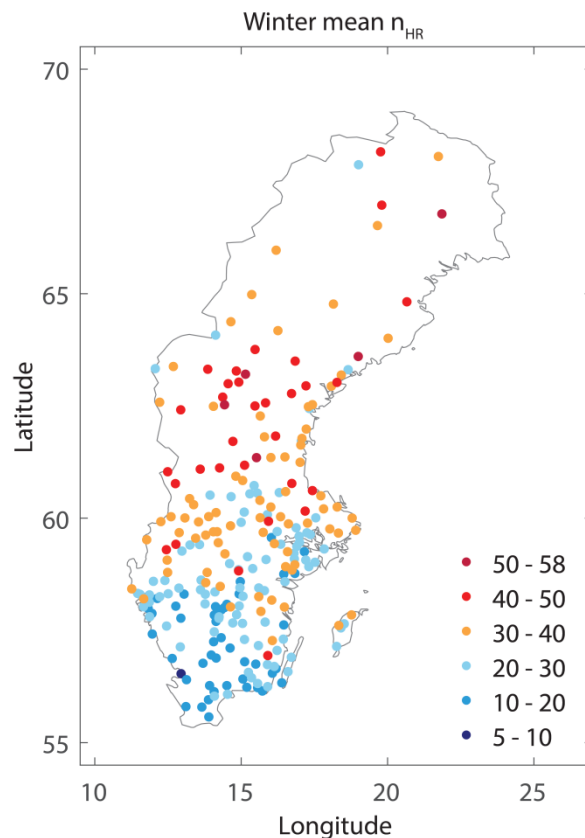


Figure 11. The average number of road hoar frost risk days ( $n_{HR}$  in days) over the 17 winters between 2000 and 2016. Figure source: Paper III (modified).

## Characteristics

In wintertime, hoar frost is seen over the whole of Sweden (Figure 11). The winter mean  $n_{HR}$  over 17 winters is lower in southern Sweden than elsewhere in the country. The most frequent occurrences of hoar frost were found in the central part of Sweden between  $61^{\circ}\text{N}$  and  $64^{\circ}\text{N}$ .

The climate background for the occurrence of hoar frost differs in different regions in Sweden (Figure 12). In northern Sweden, hoar frost usually occurs when the temperature is higher than normal, whereas it is likely to occur in the southern part of Sweden when the temperature is lower than usual. RH is generally higher when hoar frost occurs. Central Sweden seems to be a transition region, in which different spatial patterns between RST and  $T_a$  were found.

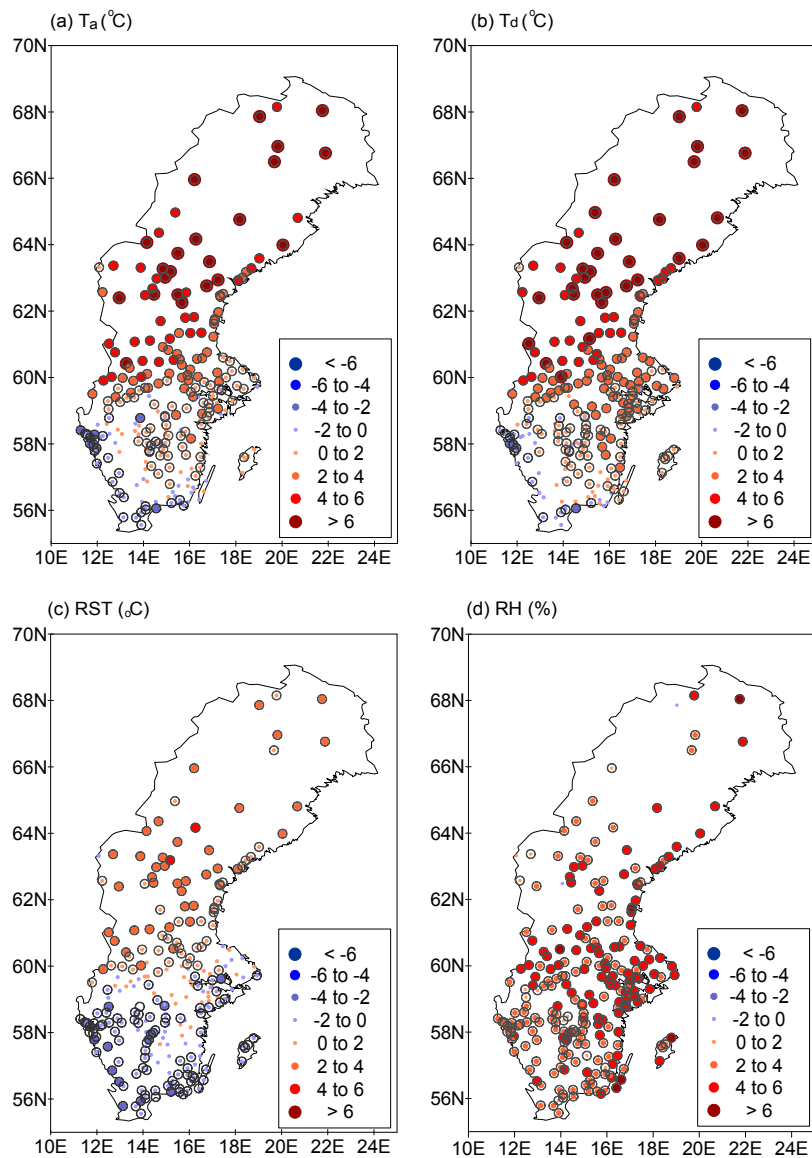


Figure 12. Difference in observed daily mean (a)  $T_a$ , (b)  $T_d$ , (c) RST and (d) RH for days with and without a hoar frost risk ( $t$ -test has been unitized, the black circles indicate the difference is significant at 0.01 level). Figure source: Paper IV.

## Classification

Based on the variation of  $T_a$  and RST shown in Figures 12(a) and 12(c), the RWIS stations were further classified into three climate zones using K-means cluster analysis (Figure 13) in Paper IV. Cluster 1 (northern Sweden) corresponds roughly to the geographic location of traditional climate zones of Lower Northern and Upper Northern Sweden; cluster 2 to Central Sweden; and cluster 3 to Southern Sweden. The classification roughly fits the traditional climate zones (Wallman 2004), which were based on the length of winter season.

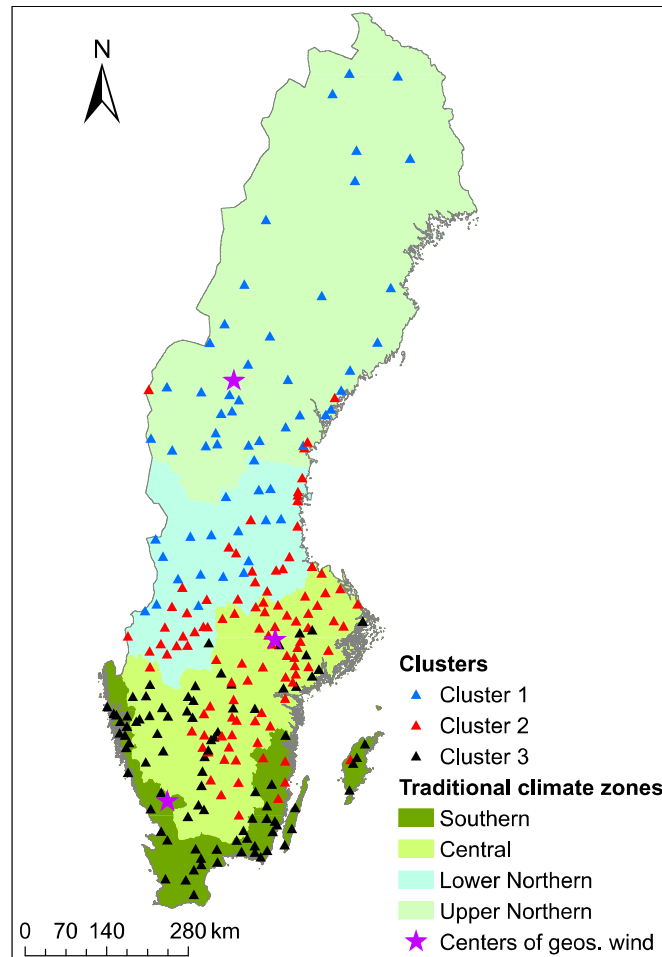


Figure 13. Locations of in situ RWIS stations and their respective clusters, and the centres of Lamb classification calculation for three region. Figure source: Paper IV.

For each classified climate zone, changes in mean temperatures (RST,  $T_a$ , and  $T_d$ ) over time with respect to the occurrence of hoar frost were investigated (Figure 14). It was found that changes in mean temperatures in northern Sweden were typical for hoar frost caused by warm air advection (e.g. Gustavsson, 1991). While in southern Sweden, a typical temperature pattern for hoar frost due to radiative cooling (e.g. Karlsson, 2001) was identified. Central Sweden is located in a transition zone between northern and southern Sweden and no clear information of the dominating hoar frost type could be identified from the mean condition.

Furthermore, occurrences of hoar frost in each climate zone were classified into four groups (Figure 15), comprising the warm air advection group (IAIR), the morning heating of air

temperature but still cold road surface group (IADR), the radiative cooling group (DADR) and the unclassified group (UC). The majority of hoar frost in Sweden is due to warm air advection and radiative cooling, with 10% of hoar frost was caused by morning heating of air temperature but cold road surface. In northern Sweden, hoar frost is mainly due to warm air advection, while hoar frost in southern Sweden is mainly caused by radiative cooling, with some caused by warm air advection. Central Sweden is located in a transition zone between northern and southern Sweden where the difference between the frequencies of the two types of hoar frost is smaller compared to that of the other two regions. Although most of the hoar frost cases could be classified into the three categories, about 30% of the hoar frost occurrences could not be classified.

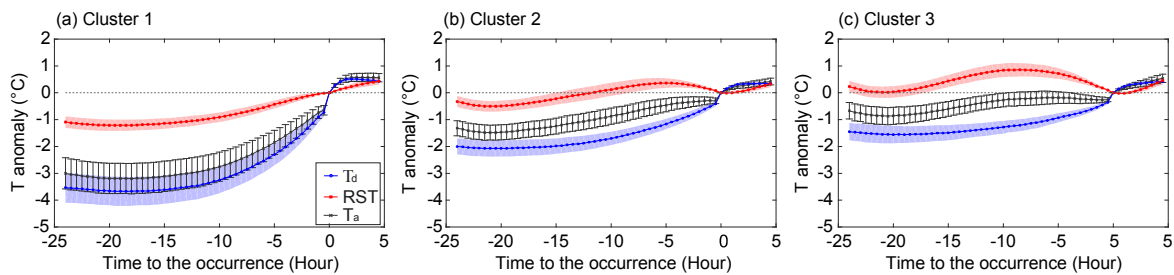


Figure 14. Mean  $T_d$ , RST, and  $T_a$  from 24 hours before to 4 hours after hoar frost for stations in (a) Northern Sweden – cluster 1, (b) Southeast and central Sweden – cluster 2, and (c) Southwest Sweden – cluster 3 ( $\pm 0.5$  standard deviation is included). Figure source: Paper IV.

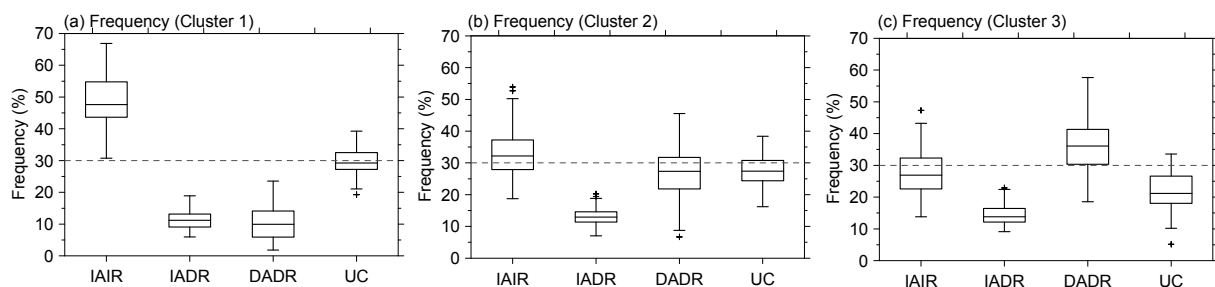


Figure 15. Box-whisker plot of the relative frequency of four different groups of hoar frost by regional cluster. Figure source: Paper IV.

## Decadal changes

In Paper III, changes in the winter  $n_{HR}$  were further examined over the period 2000 – 2016 and were found to have a strong regional pattern (Figure 16). There is a decreasing trend of winter  $n_{HR}$  in the southern part (south of  $59^\circ\text{N}$ ) and northern parts of Sweden (north of  $65^\circ\text{N}$ ), while a general increasing trend can be seen for the majority of stations in the central part of Sweden ( $59^\circ\text{N} \sim 65^\circ\text{N}$ ). The increases are often found in regions where the hoar frost risk is relatively high, while the decreases are often found in regions where the hoar frost risk is relatively low.

## Link with the recent atmospheric circulation changes

Further analysis in Paper III found that the increase in the winter  $n_{HR}$  in central Sweden ( $59^\circ\text{N} \sim 65^\circ\text{N}$ ) is mainly caused by the increase in RH, while the decrease in the winter  $n_{HR}$  in the



southern part (south of 59°N) is mainly caused by the decreased frequency with which RST is less than or equal to 0 (the prerequisite for the appearance of dangerous hoar frost conditions on road surfaces).

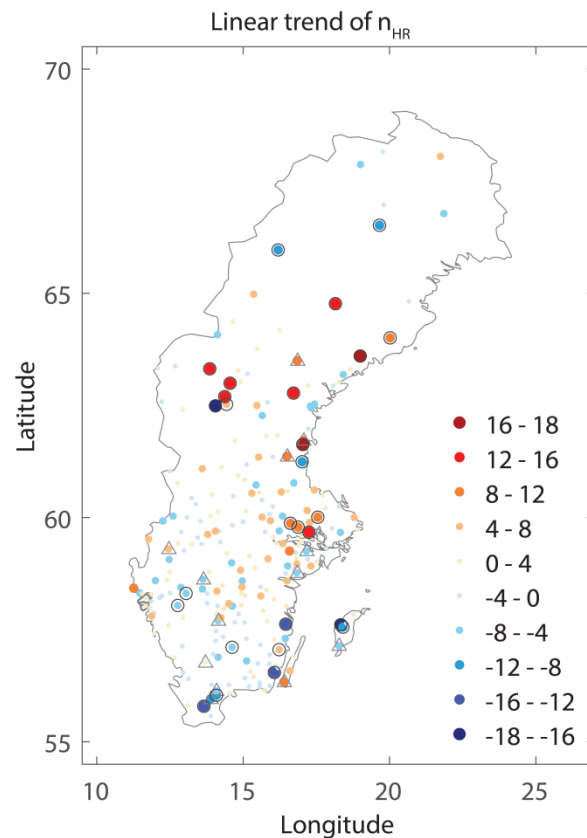


Figure 16. The linear trends of  $n_{HR}$  (days/10yr) over the 17 winters between 2000 and 2016. Stations marked with a black circle are statistically significant at  $p < 0.05$  level; stations marked with a grey triangle are statistically significant at  $p < 0.1$  level. Figure source: Paper III.

All the changes were related to the strengthened NAO over the last few decades. In the central and northern parts of Sweden, there tends to be more hoar frost risk days during the years with positive NAO, and vice versa (Figure 17), due to more water vapour being transported to Sweden in stronger NAO years compared to weaker NAO years (Figure 18(a)). This resulted in an increase in the relative humidity measured by most of the stations. Such an increase is expected to increase the risk of hoar frost, provided there is little change in the temperature. However, in the south-eastern part of Sweden, the positive relationship between the winter  $n_{HR}$  and the NAO is less pronounced and the winter  $n_{HR}$  even decreases with the strengthened NAO in the south-west part of Sweden, due to the relatively high RST in the region. The decreased number of days with blocking anticyclones (Figure 18(b)) led to less cold air transport from the north-west and more warm air from the south-west transported to Sweden. The warm air transported to the southern part of Sweden may reduce the likelihood of RST being sub-zero for a prolonged period of time thereby limiting the formation of hoar frost in the region.

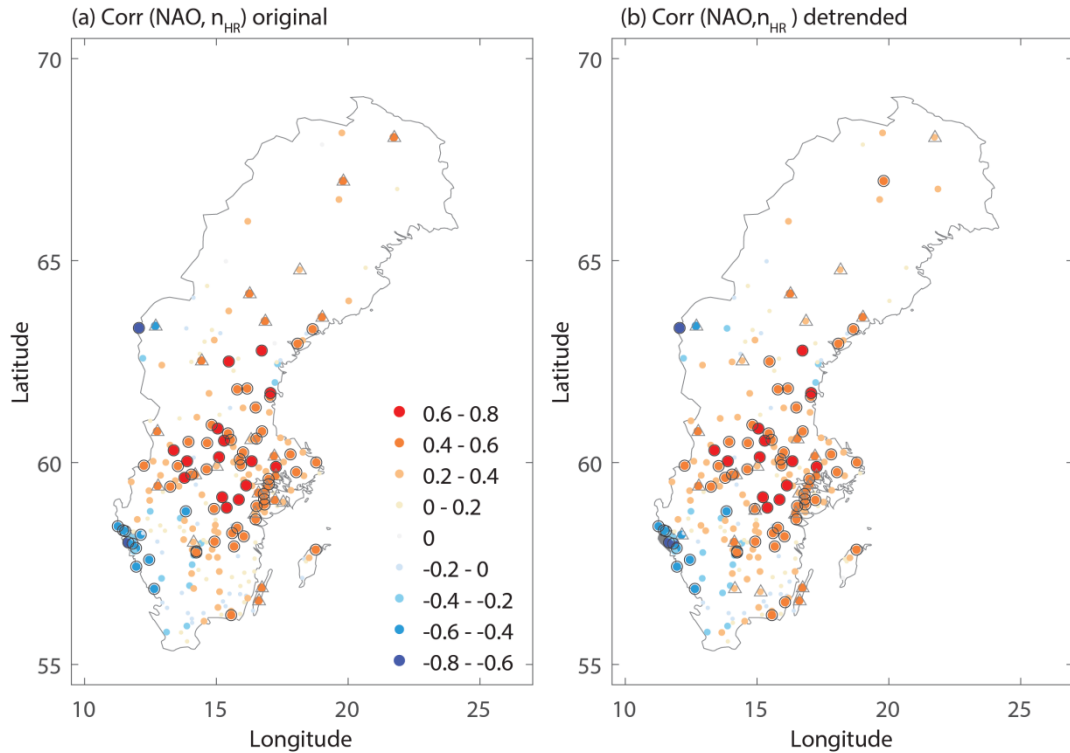


Figure 17. (a) Spatial distribution of correlation coefficient between winter (Dec-Jan-Feb) mean NAO index and the number of hoar frost risk days ( $n_{HR}$ ), (b) same as in (a) but with the linear trend of NAO index and  $n_{HR}$  removed. Stations marked with a black circle are statistically significant at  $p < 0.05$  level; stations marked with a grey triangle are statistically significant at  $p < 0.1$  level. Figure source: Paper III .

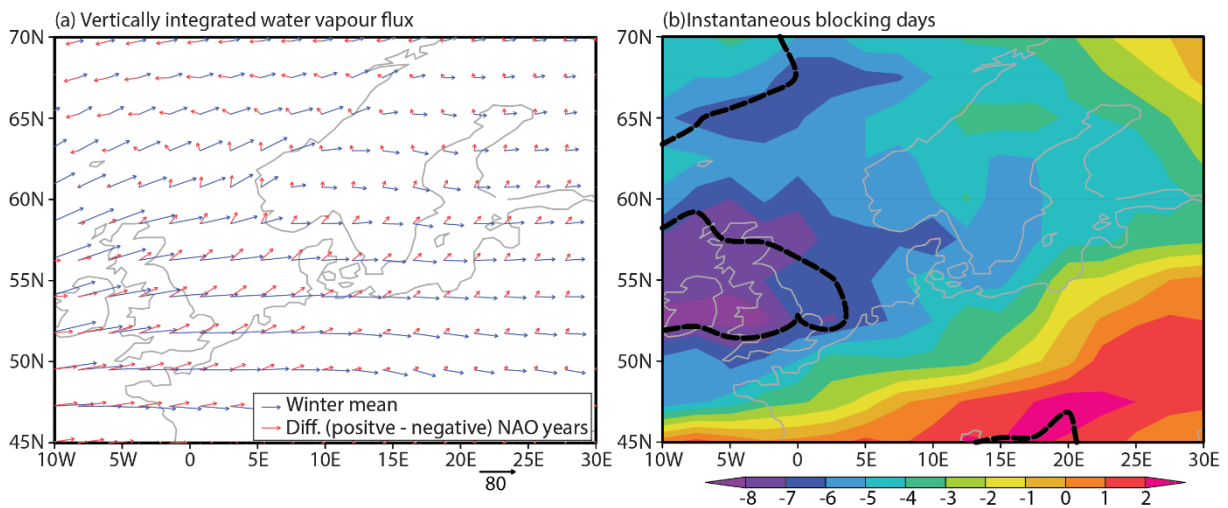


Figure 18. Composite maps for the spatial distribution of the differences of (a) the vertically integrated water vapour flux (units:  $kg \cdot m^{-1} \cdot s^{-1}$ ) and (b) instantaneous blocking days between strong positive NAO winters (winter mean NAO index  $> 0.4$  i.e. 2000, 2005, 2012, 2014, 2015, 2016) and strong negative winter NAO years winters (winter mean NAO index  $< -0.4$  i.e. 2009, 2010, 2011). In (b), the dashed line shows the region where it is significant at 0.05 level. (The ERA-Interim data have been used for the calculation. The vertically integrated water vapour

flux is calculated the same way as described in the work by Ou et al. (2011) but with the water vapour flux integrated from surface to 1mb. Instantaneous blocking days are defined as described by Davini et al. (2014) but with an additional constraint that the extent should cover at least 15° of continuous longitude, which fits the definition.). Figure source: Paper III.

## Influence of climate change on the causes of hoar frost

In the context of climate change, the possible changes in the four groups of hoar frost (IAIR, IADR, DADR and UC) were also examined in Paper IV (Figure 19). It is shown that the relative frequency of hoar frost due to warm air advection significantly decreased in relation to the increase in the large-scale  $T_a$ , while that of radiative cooling increased. No significant trend is found for the second group (morning heating of air temperature but cold road surface).

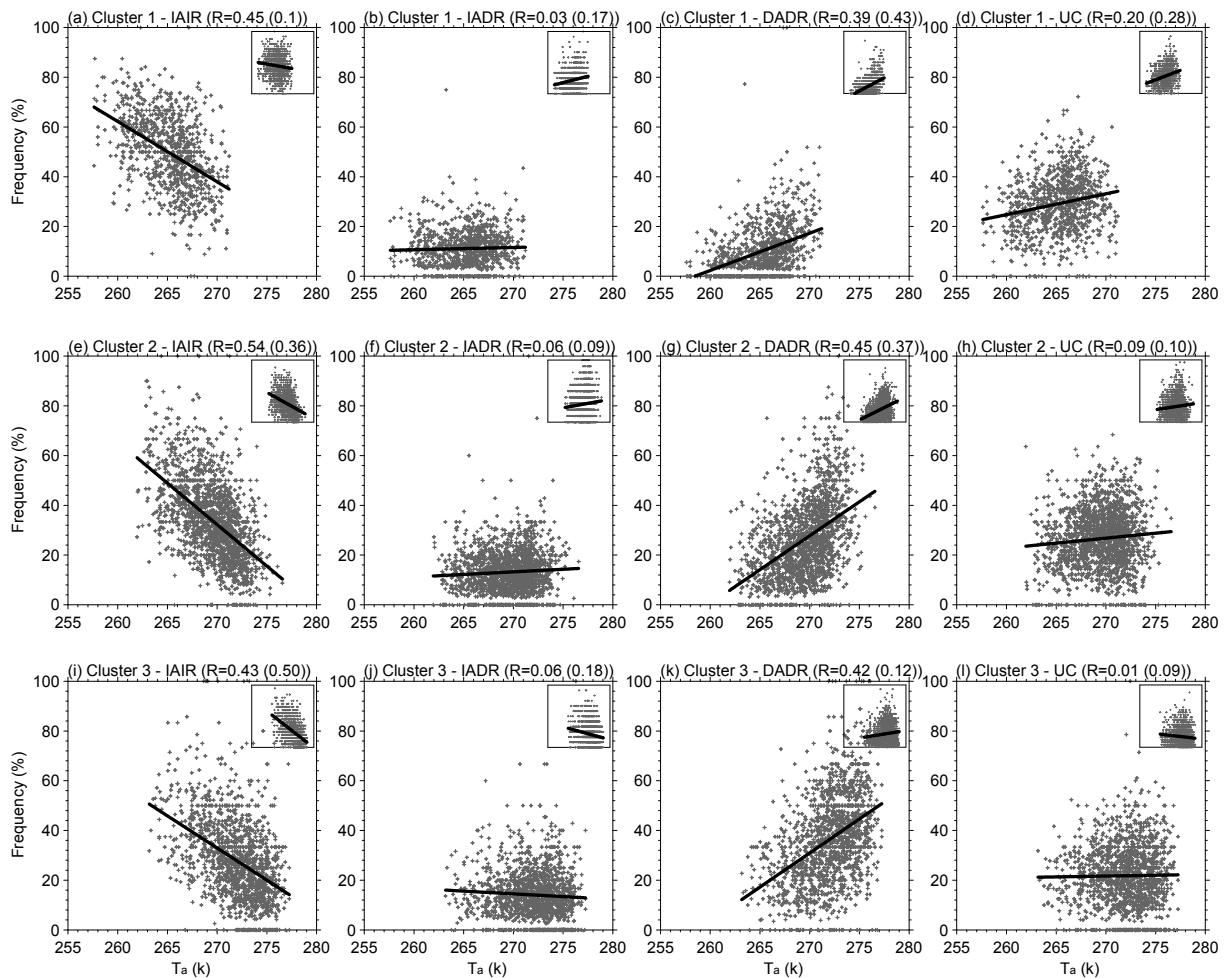


Figure 19. Link between winter mean grid temperature from MERRA2 and the relative frequency (ratio between the occurrence of each group and the total occurrence) of hoar frost in four different groups for 17 winters of each station over three regions (clusters) (the link between the occurrence and the temperature is shown in the small figure to the top-right of each figure). Figure source: Paper IV.

Further analysis showed that the weakened temperature gradient in direction west and southwest between land and ocean caused the decrease in the warm air advection type of hoar

frost, since the land temperature increases faster than that of the ocean in a warming climate (e.g. Sutton *et al.*, 2007).

## DISCUSSION

### INFLUENCE OF GEOGRAPHICAL PARAMETERS ON RST DISTRIBUTION

The radiation models that account for the influence of shading and/or  $\psi_s$  in Paper I and the geographical models built in Paper II, explained the variations of route-based RST to a large extent, which suggests that the relationship between geographical parameters and thermal mapping from times of day other than the latter part of the night can indeed be used to improve the modelling of RST variation across a road network.

#### Using screening effects in modelling route-based daytime RST

At present, daytime RST modelling is in many cases performed by interpolating data gathered from adjacent RWIS stations. However, the close correlation between the  $I$  values computed using Lidar-derived shading effects and experimentally measured RST distributions (Table 3) suggest that Lidar data may be generally useful for estimating shading patterns, thereby offering a significant increase in the accuracy of RST modelling (in comparison to simple interpolation). The general radiation model explains up to 70% of the RST distribution variance. Such good agreement between the model output and observation is remarkable and strongly suggests the method is physically reliable. Moreover, in comparison to the existing method of calculating the shading effect from fish-eye images (Chapman *et al.*, 2001b), using Lidar to derive shading effects significantly reduces the time, effort and cost for field measurements. Therefore, it may well be feasible to apply this approach on a national scale by using GIS in conjunction with DSM data.

The inclusion of  $\psi_s$  in the cumulative total incoming radiation and  $Q^*$  model explained the early morning and late afternoon RST distributions in the country road area better than the cumulative  $I$  model, due to the weak incoming  $I$  and dominating influence of long-wave and diffuse radiation during these periods. This indicates that  $\psi_s$  might be used to improve the modelling of RST variation in the early morning and late afternoon, and in more cloudy conditions.

Nevertheless, the three different radiation models described in this thesis explained quite similar proportions of the overall variation in RST for most of the measurements, especially under clear conditions. This is notable because the models are constructed in rather different ways. For the  $I$  model, only  $S_r$  needs to be considered, whereas the other two both require the calculation of  $\psi_s$  (which adds complexity to the model as calculation of  $\psi_s$  is time-consuming when dealing with large areas) and that of several other radiation fluxes. In addition, the  $Q^*$  model requires RST (here it was interpolated from nearby RWIS stations) to calculate the outgoing longwave radiation. Therefore, there is a trade-off between the higher explained variance achieved with the total incoming radiation or  $Q^*$  models and the much simpler  $I$  model. For clear conditions when the influence of  $I$  is strong, the  $I$  model is recommended.

## **Attempt to utilize FCD to reflect route-based RST distribution**

In Paper II, the repeatability of thermal fingerprints and the stable relationship between RST and geographical parameters in different families both imply that it is possible to build a geographical model based on sufficient thermal mapping data recorded over time with relatively high traffic volumes and different weather patterns. In this way, the weather forecast may be significantly improved for times of day when most daily traffic occurs and under different weather patterns. Hence, more road users will benefit from it.

However, the use of thermal mapping surveys undertaken at times of day other than the latter part of the night also introduces uncertainty into the results. Previous studies have shown that traffic generally increases RST (e.g. Farmer and Tonkinson, 1989; Chapman and Thornes, 2005). Due to the difference in traffic volume, it is expected that the influence of traffic on RST is much greater for thermal mapping surveys undertaken at times of day other than the latter part of the night than the more commonly used data recorded during the latter part of the night. Since traffic volume across a road network differs with weather conditions, time of day and time of week, it is difficult to quantify the influence of traffic. In particular, it is extremely unlikely that two thermal mapping surveys can be carried out with exactly the same traffic conditions. The random variation of RST caused by the presence of traffic is difficult to separate from other processes. For instance, Chapman and Thornes (2005) found that the influence of traffic on RST is largest during neutral nights (cloudy or windy conditions), which is similar to the weather conditions shown in group 7. The dominating influence of urban density in group 7 might be a combined effect of urban heat island and traffic. In addition, the strong influence of traffic on RST under neutral conditions also makes it difficult to quantify the influence of other geographical parameters. Besides, the frequent presence of traffic can also make it difficult to capture repeatable thermal fingerprints with only a few thermal mapping surveys under the same weather conditions at the same time of day; therefore, more thermal mapping surveys may be needed. Further investigation is needed to separate the influence of traffic from the influence of geographical parameters.

In contrast to RST, the results associated with the repeatability of  $T_a$  and the stability of the relationships between geographical parameters and  $T_a$  were not as encouraging. This is caused by the large heat capacity difference between air and the roadbed (Oke, 1987). To increase air and road surface temperatures by the same magnitude, the road surface requires much more heat than the air. Therefore, the air temperature reacts more quickly to weather changes than the temperature of the roadbed. However, since the road emits and absorbs more radiation, the RST will change more than  $T_a$  due to differences in shading and  $\psi_s$ . As mentioned above, some measurements were recorded during quite different weather patterns compared to the others in the same group, which resulted in the different spatial patterns of  $T_a$ . Due to the low heat capacity of air, the influence of earlier weather conditions on  $T_a$  was quite limited, while its influence on RST was often large.

Although the repeatability of thermal fingerprints was good and the relationship between RST and geographical parameters was stable, there are some indications that it is difficult to build a geographical model for road weather forecasting using  $T_a$  from the FCD. The main problem is the unstable relationship between  $T_a$  and geographical parameters. The influence of altitude and

urban density on RST may be reflected in the relationship between  $T_a$  and geographical parameters; however, the influences of  $\psi_s$  and shading are not pronounced, due to the difference in heat capacity between air and the roadbed. Nevertheless, the influence on RST from  $\psi_s$  and shading can be modelled reasonably well by using GIS information, as shown in Paper I; therefore, a road weather forecast model needs to take proper account of these parameters. In general, the influence of the parameters which are strongly related to RST, but not  $T_a$ , should be modelled where possible, rather than taken from the FCD. In addition, the different spatial patterns of  $T_a$  in the same group make it difficult to build a stable model. One possible way to address the differences in the values of  $T_a$  observed within the same group is to raise the cut-off for thermal fingerprint clustering, which may further divide thermal mapping surveys from different weather patterns into different groups. This may increase the similarity of  $T_a$  measurements in the same group and make it possible to model RST distribution using  $T_a$  from the FCD. However, it also means that many thermal mapping surveys will need to be performed. Further investigations are needed to better understand how best to use FCD in road weather forecasting.

## WINTER ROAD HOAR FROST RISK IN SWEDEN

In Paper III and Paper IV,  $T_a$ ,  $T_d$ , RH and the accumulation time was considered in defining hoar frost risk. As mentioned above, the influence of wind speed has been cited frequently, but it is hard to estimate the wind speed at which the deposition of hoar frost is reduced on the road surface. In this thesis, in order to cover all potentially dangerous road conditions caused by hoar frost, no upper limit was set for wind speed in the definition of hoar frost risk. Moreover, wind speed measurements recorded by RWIS stations are often problematic (Chapman *et al.*, 2001b), especially when it comes to decadal level. Of the data from 17 winters used in Paper III and Paper IV, about 30% of the wind speed data was missing. The large amount of missing data makes it difficult to evaluate the influence of wind speed on the distribution of hoar frost. Based on the available data, about 96% of measurements associated with hoar frost had a wind speed of less than or equal to 5m/s at 5m level, at which dew was still observed (Crowe *et al.*, 1978). For the other 4% of measurements with hoar frost risk identified, the amount of hoar frost deposition might be reduced due to higher wind speed, but again it is difficult to evaluate the influence since there is no clear maximum limit for wind speed from the previous studies. Nevertheless, this should not influence the results of Paper III and Paper IV, since all potentially dangerous road conditions caused by hoar frost were considered in both studies.

Figure 16 shows a very clear regional pattern of changes in winter road hoar frost risk over the last few decades, with decreasing winter  $n_{HR}$  in the southern and northern parts of Sweden and increasing winter  $n_{HR}$  in the central part of Sweden. The results indicates that hoar frost risk does not necessarily decrease in a warming climate. Given sufficient water vapour in a region, the regional hoar frost risk may increase as long as the RST is far below the freezing point. However, this was not the case for the northern part of Sweden. The hoar frost risk decreased in the region despite the slightly increased RH and low mean RST (see Paper III). This could be caused by the “snow covered” road surface conditions in the region. In Sweden, road salt is often used for de-icing in wintertime. However, a road surface with a low RST requires more salt to de-ice it than one with a higher RST. In order to minimise the usage of salt, roads in the

northern part of Sweden are often kept “winter white” with the use of road salt being infrequent (Ihs, 2002; Nordin, 2015). The “white” surface influences the RST and makes it hard to evaluate the changes in winter  $n_{HR}$  in the region.

In Paper IV, about 30% of the occurrences of hoar frost are in the unclassified group. The inability to classify these instances may be due to large variations in temperature, with some cases associated with a sudden increase in the temperature (e.g. Gustavsson, 1991), especially in the north of Sweden (e.g. Andersson et al., 2007). This may lead to the occurrence of hoar frost with a preceding period shorter than 5 hours, which cannot be classified by the current scheme. Another reason could be that the RST was around 0°C before some of the identified hoar frost (e.g. Gustavsson and Bogren, 1990). Since a minimum of 2 hours is required for the identification of hoar frost, hoar frost will not be detected if changes in RST below or above 0°C take place within 2 hours. The fluctuation of RST around 0°C makes it difficult to see any clear changes in temperature 5 hours before the identified hoar frost, making it difficult to classify the cause of such an occurrence of hoar frost.

The close relationship between NAO and the changes in hoar frost risk in Sweden suggests NAO projections could be used to predict the occurrence of hoar frost in the future. Deser *et al.* (2017) showed that NAO between 2016 and 2045 will continue to strengthen, leading to warmer winters over the whole of Sweden and wetter winters in the south-western and central to northern parts of Sweden. According to Kjellström *et al.* (2016), winter temperatures for the remainder of this century will continue to increase across the whole of Sweden, especially in the northern part. Temperatures are forecast to be higher, in comparison to the period 1971 – 2000, by up to 4 °C until 2040. It seems reasonable to expect that the warming effect will continue to dominate in the southern part of Sweden and lead to a reduction in hoar frost risk over the next 30 years. The reduction in water vapour transported to the south-eastern part of Sweden will further reduce the occurrence of hoar frost risk in the region. For the central part of Sweden, the increase in air temperature may lead to an increase in mean RST. Higher mean RSTs may lead to a decrease in the winter  $n_{HR}$  in the central part of Sweden. The reduction in water vapour transported to the eastern coast around Stockholm may further reduce the hoar frost risk in the region. However, due to the low RST and increasing water vapour in the mountainous area in the central and northern parts of Sweden,  $n_{HR}$  may continue to increase over the next 30 years. Therefore, it could be that the region with the largest mean hoar frost risk over the last few decades may see an even greater hoar frost risk and continue to be the region most affected by hoar frost over the next 30 years. Moreover, the warming may further reduce the temperature gradient between land and ocean, due to greater increases in temperature on land than in the ocean, which may lead to a decrease in the relative frequency of hoar frost due to warm air advection. However, the relative frequency of hoar frost due to radiative cooling may increase, especially in central Sweden where the total number of occurrences of hoar frost has been found to increase in a warming climate.

Results in Paper IV provide detailed insights into conditions under which hoar frost forms on roads in different climate zones. The results may be used to evaluate models for predicting hoar frost risk, which may help improve the accuracy of hoar frost prediction. Results in Paper III provide some suggestions as to the possible changes in the hoar frost risk in a warming climate,



which could be of interest to road users, WRM engineers and policymakers. The changes in hoar frost risk conditions may lead to a higher risk of traffic accidents, since people may not be used to the new winter road conditions. Using the knowledge from this study, road users could adjust their behaviour and be better prepared for future winter road conditions, thereby reducing the risk of traffic accidents. In addition, the changes in winter hoar frost risk conditions may lead to changes in WRM activities in a region (from snowploughing to salting, for example). The results could be used by WRM engineers in planning maintenance activities and the deployment of equipment. Proper preparation could reduce WRM expenditure and protect the environment by reducing the amount of salt used in WRM. Finally, the results could be of interest to transportation policy-makers when developing road-related infrastructure adaptation strategies in a changing climate.

## CONCLUSIONS

The thesis focused on the influence of geographical parameters on RST and the influence of climate change on winter road hoar frost risk. The main conclusions can be summarised as follows:

- Daytime thermal mapping combined with high resolution Lidar data can be used to build radiation models which take into account the effect of shading and  $\psi_s$ , and these models can explain daytime RST distribution up to 70%.
- Cumulative direct short-wave radiation model that consider the effect of shading is recommended for daytime RST modelling due to its simplicity. However, the influence of  $\psi_s$  should not be neglected for situations such as early morning, late afternoon or when the influence of clouds is large.
- Geographical parameters combined with thermal mapping data recorded at times of day other than the latter part of the night can be used to build repeatable geographical models and explain the RST distribution up to 67%.
- It is meaningful to use  $T_a$  from the FCD to estimate the effect of altitude and urban heat island on RST distribution. However, the influence of other parameters, such as shading and  $\psi_s$ , can not be estimated from  $T_a$  and needs to be modeled using an energy balance model.
- Hoar frost risk for winter road is mainly caused by warm air advection in northern Sweden and radiative cooling in southern Sweden.
- Over the past few decades, increased RST has led to a decreased risk of hoar frost on roads in the south of Sweden (south of 59°N), whilst increased relative humidity has led to an increased risk of hoar frost on roads in central Sweden (59°N ~ 65°N). The strengthened winter North Atlantic Oscillation (NAO) is the main cause for the changes.
- In a warming climate, the relative frequency of hoar frost under warm air advection has significantly decreased, while the relative frequency due to radiative cooling has significantly increased, mainly due to the weakened temperature gradient between land and ocean.

## ACKNOWLEDGEMENTS

The research presented in this thesis was funded by the Swedish Transport Administration. I am grateful for the financial support provided by the agency during the past few years.

I would like to thank my supervisors Torbjörn Gustavsson and Jörgen Bogren for giving me the opportunity to begin this journey and for helping me to complete it. Thank you for sharing knowledge and experience, for your support in collaboration with different researchers and groups, for your encouragements in tough moments and support with funding. To my co-supervisor Fredrik Lindberg, thank you for sharing knowledge and programming skills, which is very important for a beginner in programming.

I am especially grateful to my examiner, Prof. Deliang Chen, for various interesting discussions, constructive comments and suggestions to my work. Thank you for sharing your knowledge and experience both in research and life.

This thesis would not have been possible without the close cooperation with several researchers. To Esben Almkvist, I am grateful for your constructive instructions and your patience in the countless online discussion. Thank you for sharing knowledge, programming skills and research experience with me. I am especially grateful to you for reading and giving constructive suggestions on my thesis in the last moment. To Jianbin Huang, thank you for always encouraging me to present my work and for giving me valuable suggestions on both presenting and writing skills. I will remember the morning walks to GVC, during which we had various discussions and I surely benefited from that. To Tinghai Ou, thank you for your constant support, constructive suggestions, patience and encouragement during this journey.

This project started with a steering group of people from different areas of interest. To Håkan Westerlund, Pontus Gruhs, Pertti Kuusisto, Ander Jandel, Andreas Bäckström, Karim Hawzheen, Henrik Hansson, Anna Arvidsson and Patrik Lidström, thank you for your discussions and comments on the presentations of my work. Special thanks to Anna Arvidsson from VTI, Andreas Blomkvist, Jonas Hallenberg and Dan Eriksson from the Swedish Transport Administration, thank you for answering my questions and helping me with data downloading.

I would like to thank all my current and previous colleagues at GVC for creating such a nice working environment. Big thanks to David Rayner for reading one of my manuscript and giving constructive comments. I am grateful to Anna-Karin Björsne, Michelle Nygren and Hongxing He for constructive comments on my thesis. Special thanks to Hongxing He for your help both in research and life. To Janina Konarska, I will remember the great time when sharing office with you and thank you for all the interesting discussions and fikas. To Shiho Onomura, for always being nice to me, for sharing knowledge and life experience, for various discussions and for initiating many social activities. To Irina Polovodova Asteman, for the fikas and social activities. To Lina Nordin, for your accompany in different conferences and for encouraging me to speak Swedish. To Hans Alter, for fixing the instruments and the truck for my field measurements. To Kristina Seftigen and Jesper Björklund for being both great colleagues and friends, thank you for the fun we had together. To Changgui Lin, for the fikas in the last year and many pieces of advice. To Philipp Schleusner, for your accompany during the last few

months in thesis writing and your encouragements. To Alexander Walther, Peng Zhang, Aifang Chen, Fei Wang, Gangfeng Zhang, Lorenzo Minola and many other colleagues for creating such an inspiring and enjoyable working environment.

I also want to express my gratitude to everyone at Klimator, thank you all for the help and care during this journey. Special thanks to Eric Zachrisson, for your help with the field measurements. To Johan Edblad, for generating data after my measurements. I would also like to extend my gratitude to Ana Pérez Aponte, for your driving and accompany during those long days in the field.

I would also like to thank all my friends in Gothenburg and China. Especially to Lina Wei Zhang for sharing living experiences, for helping me in private life and for all the funs we had together. To Ge Gao for your encouragements during this journey and many nice presents from China. To Linnan Yu, for your help and the fun you brought to my private life. To Diana Wang, for the random chatting and relaxing time together, which gave me special breaks from research. To Xuefei Zhang, for the relaxing social activities we had together. To Ulrika Asztély-Nilsson and your family, for inviting me to your house during different festivals and for all those great memories.

Huge thanks to my family for their constant support, for believing in me and for their encouragements. I am especially grateful to my parents, for traveling so long distance to help me with private life. Without you, I would have never completed this journey. To my husband, for always listening to me and giving suggestions when I need advice and help. To my lovely twins, Vincent and Felicia, thank you for letting me fully relaxed from research during evenings and for making me laugh when I need it the most! I love you and I am so proud of you!

Additional financial support has been gratefully received from:

- Adlerbertska Scholarship Foundation,
- Paul and Marie Berghaus Donation Scholarship
- Professor Sven Lindqvist Research Foundation.

## REFERENCES

- Al-Qadi, I.L., Loulizi, A., Flintsch, G.W., Roosevelt, D.S., Decker, R., Wambold, J.C., Nixon, W.A., 2002. Feasibility of using friction indicators to improve winter maintenance operations and mobility. NCHRP Web Document, **53**, NCHRP Project 6-14 Contractor Final Report.
- Andersson, A., Chapman, L., 2011. The use of a temporal analogue to predict future traffic accidents and winter road conditions in Sweden. *Meteorological Applications*, **18**, 125-136.
- Andersson, A.K., Gustavsson, T., Bogren, J., & Holmer, B., 2007. Geographical distribution of road slipperiness in Sweden, on national, regional and county scales. *Meteorological Applications*, **14**, 297-310.
- Blomqvist, G., Folkesson, L., 2001. Indicators for monitoring the system of de-icing salt use and its impacts on groundwater, vegetation and societal assets. Ph. D. Thesis, Royal Institute of Technology, Stockholm. <http://www.ectri.org/YRS05/Papiers/Session-1ter/blomqvist.pdf>.
- Bogren, J., Gustavsson, T., 1991. Nocturnal air and road surface temperature variations in complex terrain. *International Journal of Climatology*, **11**, 443-455.
- Bogren, J., Gustavsson, T., Karlsson, M., 2001. Temperature differences in the air layer close to a road surface. *Meteorological Applications*, **8**, 385-395.
- Bogren, J., Gustavsson, T., Karlsson, M., Postgard, U., 2000. The impact of screening on road surface temperature. *Meteorological Applications*, **7**, 97-104.
- Brown, A., Jackson, S., Murkin, P., Sheridan, P., Skea, A., Smith, S., Veal, A., Vosper, S., 2008. New techniques for route-based forecasting. Proceedings of the 14th Standing International Road Weather Commission, Prague, Czech Republic, 14-16 May 2008 (available online).
- Bulygina, O.N., Arzhanova, N.M., & Groisman, P.Y. (2015). Icing conditions over Northern Eurasia in changing climate. *Environmental Research Letters*, **10**, 025003.
- Chapman, L., Thornes, J.E., 2005. The influence of traffic on road surface temperatures: implications for thermal mapping studies. *Meteorological Applications*, **12**, 371-380.
- Chapman, L., Thornes, J.E., 2006. A geomatics-based road surface temperature prediction model. *Science of The Total Environment*, **360**, 68-80.  
<https://doi.org/10.1016/j.scitotenv.2005.08.025>.
- Chapman, L., Thornes, J.E., 2011. What spatial resolution do we need for a route-based road weather decision support system? *Theoretical and Applied Climatology*, **104**, 551-559.
- Chapman, L., Thornes, J.E., Bradley, A.V., 2001a. Modelling of road surface temperature from a geographical parameter database. Part 1: Statistical. *Meteorological Applications*, **8**, 409-419.
- Chapman, L., Thornes, J.E., Bradley, A.V., 2001b. Modelling of road surface temperature from a geographical parameter database. Part 2: Numerical. *Meteorological Applications*, **8**, 421-436.
- Chapman, L., Thornes, J.E., Bradley, A.V., 2001c. Rapid determination of canyon geometry parameters for use in surface radiation budgets. *Theoretical and Applied Climatology*, **69**, 81-89.
- Crowe, M.J., Coakley, S.M., Emge, R.G., 1978. Forecasting Dew Duration at Pendleton, Oregon, Using Simple Weather Observations. *Journal of Applied Meteorology*, **17**, 1482-1487.
- Dai, A., 2006. Recent climatology, variability, and trends in global surface humidity. *Journal of Climate*, **19**, 3589-3606.

- Davini, P., Cagnazzo, C., Fogli, P.G., Manzini, E., Gualdi, S., & Navarra, A., 2014. European blocking and Atlantic jet stream variability in the NCEP/NCAR reanalysis and the CMCC-CMS climate model. *Climate Dynamics*, **43**, 71-85.
- Dee, D. P., Uppala, S. M., Simmons, A. J., Berrisford, P., Poli, P., Kobayashi, S., . . . Vitart, F., 2011. The ERA-Interim reanalysis: configuration and performance of the data assimilation system. *Quarterly Journal of the Royal Meteorological Society*, **137**(656), 553-597.
- Deser, C., Hurrell, J.W., & Phillips, A.S., 2017. The role of the North Atlantic Oscillation in European climate projections. *Climate Dynamics*, **49**, 3141-3157.
- Eddington, R., 2006. Transport's role in sustaining the UK's productivity and competitiveness. HMSO, London.
- Farmer, S., Tonkinson, P., 1989. Road surface temperature model verification using input data from airfields, roadside sites and the mesoscale model. UK Meteorological Office, Exeter, UK.
- Geiger, R., Aron, R.H., Todhunter, P., 1950. The climate near the ground. Rowman & Littlefield Pub Incorporated.
- Gelaro, R., McCarty, W., Suárez, M.J., Todling, R., Molod, A., Takacs, L., . . . Zhao, B., 2017. The Modern-Era Retrospective Analysis for Research and Applications, Version 2 (MERRA-2). *Journal of Climate*, **30**, 5419-5454.
- Gocheva, A., 1990. Statistical distribution of air temperature, relative humidity and wind velocity during rime-icing for the non-mountain part of the territory of Bulgaria. Proceedings of 5th International Youth School on Meteorology and Hydrology, **4**: 84-89.
- Grout, T., Hong, Y., Basara, J., Balasundaram, B., Kong, Z.Y., Bukkapatnam, S.T.S., 2012. Significant winter weather events and associated socioeconomic impacts (Federal Aid Expenditures) across Oklahoma: 2000-10. *Weather, Climate, and Society*, **4**, 48-58.
- Gustavsson, T., 1991. Analyses of local climatological factors controlling risk of road slipperiness during warm-air advections. *International Journal of Climatology*, **11**, 315-330.
- Gustavsson, T., 1999. Thermal mapping - a technique for road climatological studies. *Meteorological Applications*, **6**, 385-394.
- Gustavsson, T., Bogren, J., 1990. Road slipperiness during warm-air advections. *Meteorological Magazine*, **119**, 267-270.
- Gustavsson, T., Bogren, J., 1991. Infrared thermography in applied road climatological studies. *International Journal of Remote Sensing*, **12**, 1811-1828.
- Gustavsson, T., Bogren, J., Green, C., 2001. Road climate in Cities: A study of the Stockholm area, south-east Sweden. *Meteorological Applications*, **8**, 481-489.
- Gustavsson, T., Karlsson, M., Bogren, J., Lindqvist, S., 1998. Development of temperature patterns during clear nights. *Journal of Applied Meteorology*, **37**, 559-571.
- Hewson, T., Gait, N., 1992. Hoar frost deposition on roads. *Meteorological Magazine*, **121**, 1-21.
- Huang, J., Zhang, X., Zhang, Q., Lin, Y., Hao, M., Luo, Y., . . . Zhang, J., 2017. Recently amplified arctic warming has contributed to a continual global warming trend. *Nature Climate Change*, **7**(12), 875-879.
- Huling, E.E., Hollocher, T.C., 1972. Groundwater contamination by road salt - steady-state concentrations in East Central Massachusetts. *Science*, **176** (4032), 288-290.
- Ihs, A., 2002. Winter maintenance in Sweden. Compiled for COST 344 "Improvements to Snow and Ice Control on European Roads". VTI *särtryck 351*.

- Karlsson, I.M., 2000. Nocturnal air temperature variations between forest and open areas. *Journal of Applied Meteorology*, **39**, 851-862.
- Karlsson, M., 2001. Prediction of hoar-frost by use of a Road Weather information System. *Meteorological Applications*, **8**, 95-105.
- Kjellström, E., Barring, L., Nikulin, G., Nilsson, C., Persson, G., & Strandberg, G., 2016. Production and use of regional climate model projections – A Swedish perspective on building climate services. *Climate Services*, **2**, 15-29.
- Knollhoff, D.S., Takle, E.S., Gallus, W.A., Burkheimer, D., McCauley, D., 2003. Evaluation of a frost accumulation model. *Meteorological Applications*, **10**, 337-343.
- Landelius T., Josefsson W., Persson T., 2001. "SMHI (STRÅNG): A system for medlling solar radiation parameters with mesoscale spatial resolution". SMHI Reports. RMK. No. 96
- Lindqvist, S., 1975. Våghalkans beroende av mikro- och lokalklimatiska faktorer. Department of Physical Geography, Gothenburg, 41 pp.
- Lindqvist, S., 1976. Methods for detecting road sections with high frequency of ice formation. Department of Physical Geography, Gothenburg, *GUNI rapport*, **10**, p. 32 pp.
- Lindqvist, S., 1979. Studies of slipperiness on roads. *GUNI Report*, **12**, Dept. of Physical Geography, Gothenburg, 46 pp. (in Swedish with English abstract).
- Lindqvist, S., Mattsson, J.O., 1979. Climatic background factors for testing an ice-surveillance system. *GUNI Rapport*, **13**. 35 pp.
- Milloy, M., Humphreys, J., 1969. The influence of topography on the duration of ice-forming conditions on a road surface. RRL Report. Ministry of Transport, Crothorne.
- Moore, D.F., 1975. The friction of pneumatic tyres. Elsevier Scientific, Oxford, 220pp.
- Nordin, L., 2015. Energy efficiency in winter road maintenance-a road climatological perspective. Department of Earth Sciences, University of Gothenburg.
- Norrman, J., 2000. Slipperiness on roads - an expert system classification. *Meteorological Applications*, **7**, 27-36.
- Norrman, J., Eriksson, M., Lindqvist, S., 2000. Relationships between road slipperiness, traffic accident risk and winter road maintenance activity. *Climate Research*, **15**, 185-193.
- Oke, T.R., 1987. Boundary layer climates. Psychology Press.
- Ou, T., Liu, Y., Chen, D., Rayner, D., Zhang, Q., Gao, G., Xiang, W., 2011. The influence of large-scale circulation on the summer hydrological cycle in the Haihe River basin of China. *Acta Meteorol Sin*, **25**, 517.
- Riehm, M., Nordin, L., 2012. Optimization of winter road maintenance energy costs in Sweden: a critique of site specific frost warning techniques. *Meteorological Applications*, **19**, 443-453.
- Shao, J., Lister, P., Hart, G., Pearson, H., 1996. Thermal mapping: reliability and repeatability. *Meteorological Applications*, **3**, 325-330.
- Shao, J., Swanson, J.C., Patterson, R., Lister, P.J., McDonald, A.N., 1997. Variation of winter road surface temperature due to topography and application of Thermal Mapping. *Meteorological Applications*, **4**, 131-137.
- Simmons, A.J., Willett, K.M., Jones, P.D., Thorne, P.W., & Dee, D.P., 2010. Low-frequency variations in surface atmospheric humidity, temperature, and precipitation: Inferences from reanalyses and monthly gridded observational data sets. *Journal of Geophysical Research*, **115**, D01110.

- SMHI., 2017. Sveriges klimat har blivit varmare och blötare.  
<https://www.smhi.se/kunskapsbanken/klimat/sveriges-klimat-har-blivit-varmare-och-blotare-1.21614>. Accessed 13 March 2018.
- Stocker T.F., Qin, D., Plattner, G.-K., Alexander, L.V., Allen, S.K., Bindoff, N.L., . . . Midgle, P.M. (2013). Technical summary. In: Climate change 2013: the physical science basis. Contribution of Working Group I to the Fifth Assessment Report of the Intergovernmental Panel on Climate Change. Cambridge University Press, Cambridge, United Kingdom and New York, NY, USA.
- Stull, R., 2000. Meteorology for scientists and engineers. Brooks/Cole.
- Sutton, R.T., Dong, B., Gregory, J.M., 2007. Land/sea warming ratio in response to climate change: IPCC AR4 model results and comparison with observations. *Geophysical Research Letters*, **34**.
- Swedish Transport Administration. (2015). The Swedish Transport Administration Annual Report 2014. Publikation 2015,056. Borlänge.
- Swedish Transport Administration. (2016). The Swedish Transport Administration Annual Report 2015. Publikation 2016,053. Borlänge.
- Swedish Transport Administration. (2017). The Swedish Transport Administration Annual Report 2016. Publikation 2017,095. Borlänge.
- Tabony, R.C., 1985. The variation of surface temperature with altitude. *Meteorological Magazine*, **114**, 37-48.
- Takle, E.S., 1990. Bridge and roadway frost: occurrence and prediction by use of an expert system. *Journal of Applied Meteorology*, **29**, 727-734.
- Thornes, J.E., 1991. Thermal mapping and road-weather information systems for highway engineers. *Highway Meteorology*, 39-67.
- Toms, B.A., Basara, J.B., Hong, Y., 2017. Usage of existing meteorological data networks for parameterized road ice formation modeling. *Journal of Applied Meteorology and Climatology*, **56**, 1959-1976.
- Wallman, C.-G., 2004. The Winter Model: a winter maintenance management system. In Transportation Research Circular E-C063, Transportation Research Board, National Research Council, Washington, D.C., pp. 83–94.
- Wallman, C.-G., Åström, H., 2001. Friction measurement methods and the correlation between road friction and traffic safety. A literature review., VTI MEDDELANDE, p. 47.
- White, S.P., Thornes, J.E., CHAPMAN, I., 2006. A guide to road weather systems. SIRWEC.
- Wilks, D.S., 2011. Statistical methods in the atmospheric sciences. 3rd Edition. Academic Press.